Kondo quantum dot coupled to ferromagnetic leads: a study by numerical renormalization group technique

M. Sindel,[1] L. Borda,[1,2] J. Martinek,[3,4,5] R. Bulla,[6] J. König,[7] G. Schön,[5] S. Maekawa,[3] and J. von Delft[1]
[1] *Physics Department, Arnold Sommerfeld Center for Theoretical Physics, and Center for NanoScience, Ludwig-Maximilians-Universität München, 80333 München, Germany*
[2] *Research Group "Theory of Condensed Matter" of the Hungarian Academy of Sciences, TU Budapest, H-1521, Hungary*
[3] *Institute for Materials Research, Tohoku University, Sendai 980-8577, Japan*
[4] *Institute of Molecular Physics, Polish Academy of Sciences, 60-179 Poznań, Poland*
[5] *Institut für Theoretische Festkörperphysik and DFG-Center for Functional Nanostructures (CFN), Universität Karlsruhe, D-76128 Karlsruhe, Germany.*
[6] *Theoretische Physik III, Elektronische Korrelationen und Magnetismus, Universität Augsburg, Augsburg, Germany*
[7] *Institut für Theoretische Physik III, Ruhr-Universität Bochum, 44780 Bochum, Germany*

(Dated: February 1, 2008)

We systematically study the influence of ferromagnetic leads on the Kondo resonance in a quantum dot tuned to the local moment regime. We employ Wilson's numerical renormalization group method, extended to handle leads with a spin asymmetric density of states, to identify the effects of (i) a finite spin polarization in the leads (at the Fermi-surface), (ii) a Stoner splitting in the bands (governed by the band edges) and (iii) an arbitrary shape of the leads density of states. For a generic lead density of states the quantum dot favors being occupied by a particular spin-species due to exchange interaction with ferromagnetic leads leading to a suppression and splitting of the Kondo resonance. The application of a magnetic field can compensate this asymmetry restoring the Kondo effect. We study both the gate-voltage dependence (for a fixed band structure in the leads) and the spin polarization dependence (for fixed gate voltage) of this compensation field for various types of bands. Interestingly, we find that the full recovery of the Kondo resonance of a quantum dot in presence of leads with an energy dependent density of states is not only possible by an appropriately tuned external magnetic field but also via an appropriately tuned gate voltage. For flat bands simple formulas for the splitting of the local level as a function of the spin polarization and gate voltage are given.

PACS numbers: 75.20.Hr, 72.15.Qm, 72.25.-b, 73.23.Hk

I. INTRODUCTION

The interplay between different many-body phenomena, such as superconductivity, ferromagnetism, or the Kondo effect, has recently attracted a lot of experimental and theoretical attention. A recent experiment of Buitelaar[1] *et al.* nicely demonstrated that Kondo correlations compete with superconductivity in the leads. The interplay between Kondo correlations and itinerant electron ferromagnetism in the electrodes, has theoretically been intensively studied within the last years,[2–9] initially leading to controversial conclusions.

For effectively single-level quantum dots (i.e. dots with a level spacing much bigger than the level broadening Γ), consensus was found that a finite spin asymmetry in the density of states in the leads results (in general) in a splitting and suppression of the Kondo resonance. This is due the spin dependent broadening and renormalization of the dot level position induced by spin-dependent quantum charge fluctuations. In terms of the Kondo spin model it can be treated as an effective exchange interaction between a localized spin on the dot and ferromagnetic leads. Moreover, it was shown that a strong coupling Kondo fixed point with a reduced Kondo temperature can develop[6,7] even though the dot is coupled to ferromagnetic leads, given an external magnetic field[6] or electric field[7] (gate-voltage) is tuned appropriately. Obviously, in the limit of fully spin polarized leads, when only one spin component is present for energies close to Fermi surface (half-metallic leads), the effective screening of the impurity *cannot* take place any more and the Kondo resonance does *not* develop. A part of these theoretical predictions have recently been confirmed in an experiment by Pasupathy[10] *et al.* The presence of ferromagnetic leads could also nicely explain the experimental findings of Nygård[11] *et al.*

Since the interplay between ferromagnetism and strong correlation effects is one of the important issues in spintronics applications, there are currently many research activities going on in this direction. The goal is to manipulate the magnetization of a local quantum dot (i.e. its local spin) by means of an external parameter, such as an external magnetic field or an electric field (a gate voltage), with a high accuracy. This would provide a possible method of writing information in a magnetic memory.[12] Since it is extremely difficult to confine a magnetic field such that it only affects the quantum dot under study, it is of big importance to search for alternative possibilities for such a manipulation (e. g. by means of a local gate-voltage as proposed by the authors[13]).

In this paper we push forward our previous work by performing a systematic analysis on the dependence of physical quantities on different band structure properties. Starting from the simplest case we add the ingre-

dients of a realistic model one-by-one allowing a deeper understanding of the interplay of Kondo model and itinerant electron ferromagnetism. In this paper we extend our recent studies carried out in this direction[6,7,13] and illustrate the strength of the analytical methods by comparing the results predicted by them to the results obtained by the exact numerical renormalization group (NRG) method.[14] While in Refs.[2–9] the dot was attached to ferromagnetic leads with an unrealistic, spin-independent and flat band - with a spin-dependent tunneling amplitude - we generalize this treatment here by allowing for arbitrary density of states (DOS) shapes.[13] In particular, we carefully analyze the consequences of typical DOS shapes in the leads on the Kondo resonance. We explain the difference between these shapes and provide simple formulas (based on perturbative scaling analysis[15,16]) that explain the numerical results analytically.

We study both the effect of a finite leads spin polarization *and* the gate voltage dependence of a single-level quantum dot contacted to ferromagnetic leads with three relevant DOS classes: (i) for flat bands without Stoner-splitting, (ii) for flat bands with Stoner-splitting and (iii) for an energy dependent DOS (also including Stoner-splitting). For this sake we employ an extended version of the NRG method to handle arbitrary shaped bands.[17]

The article is organized as follows: In Sec. II we define the model Hamiltonian of the quantum dot coupled to ferromagnetic leads. In Sec. III we explain details of the Wilson's mapping on the semi-infinite chain in the case of the spin-dependent density of states with arbitrary energy dependence. Using the perturbative scaling analysis we give prediction for a spin-splitting energy for various band shapes in Sec. IV. In Sec. V the results for spin-dependent flat DOS are demonstrated together with the Friedel sum rule analysis. The effect of the Stoner splitting is discussed in Sec. VI together with comparison to experimental results from Ref.[11] and an arbitrary band structure in Sec. VII. We summarize our findings then in Sec. VIII.

II. MODEL: QUANTUM DOT COUPLED TO FERROMAGNETIC LEADS

We model the problem at hand by means of a single-level dot of energy $\epsilon_{\rm d}$ (tunable via an external gate-voltage $V_{\rm G}$) and charging energy U that is coupled to identical, noninteracting leads (in equilibrium) with Fermi-energy $\mu = 0$. Accordingly the system is described by the following Anderson impurity model

$$\begin{aligned} \hat{\mathcal{H}} &= \hat{\mathcal{H}}_\ell + \hat{\mathcal{H}}_{\ell d} + \hat{\mathcal{H}}_d \,, \\ \hat{\mathcal{H}}_d &= \epsilon_{\rm d} \sum_\sigma \hat{n}_\sigma + U \hat{n}_\uparrow \hat{n}_\downarrow - B S_z \,, \end{aligned} \tag{1}$$

with the lead and the tunneling part of the Hamiltonian

$$\hat{\mathcal{H}}_\ell = \sum_{rk\sigma} \epsilon_{rk\sigma} c^\dagger_{rk\sigma} c_{rk\sigma} \,, \tag{2}$$

$$\hat{\mathcal{H}}_{\ell d} = \sum_{rk\sigma} (V_{rk} d^\dagger_\sigma c_{rk\sigma} + \text{h.c.}) \,. \tag{3}$$

Here $c_{rk\sigma}$ and d_σ ($\hat{n}_\sigma = d^\dagger_\sigma d_\sigma$) are the Fermi operators for electrons with momentum k and spin σ in lead r ($r =$ L/R) and in the dot, respectively. The spin-dependent dispersion in lead r, parametrized by $\epsilon_{rk\sigma}$, reflects the spin-dependent DOS, $\rho_{r\sigma}(\omega) = \sum_k \delta(\omega - \epsilon_{rk\sigma})$, in lead r; *all* information about energy and spin dependency in lead r is contained in the dispersion function $\epsilon_{rk\sigma}$. V_{rk} labels the tunneling matrix-element between the impurity and lead r, $S_z = (\hat{n}_\uparrow - \hat{n}_\downarrow)/2$, and the last term in Eq. (1) denotes the Zeeman energy due to external magnetic field B acting on the dot spin only. Here we neglect the effect of an external magnetic field on the leads' electronic structure as well as a stray magnetic field from the ferromagnetic leads. The coupling between the dot level and electrons in lead r leads to a broadening and a shift of the level $\epsilon_{\rm d}$, $\epsilon_{\rm d} \to \tilde{\epsilon}_{\rm d}$ (where the tilde denotes the renormalized level). The *energy* and *spin* dependency of the broadening and the shift, determined by the coupling, $\Gamma_{r\sigma}(\omega) = \pi \rho_{r\sigma}(\omega) |V_r(\omega)|^2$, plays the key role in the effects outlined in this paper. Henceforth, we assume V_{rk} to be real and k-independent, $V_{rk\sigma} = V_r$, and lump all energy and spin-dependence of $\Gamma_{r\sigma}(\omega)$ into the DOS in lead r, $\rho_{r\sigma}(\omega)$.[18]

Without loosing generality we assume the coupling to be symmetric, $V_{\rm L} = V_{\rm R}$. Accordingly, by performing a unitary transformation[19] $\hat{\mathcal{H}}_\ell$ simplifies to $\hat{\mathcal{H}}_\ell = \frac{1}{2} \sum_{k\sigma} (\epsilon_{{\rm L}k\sigma} + \epsilon_{{\rm R}k\sigma}) \, \alpha^\dagger_{sk\sigma} \alpha_{sk\sigma}$, where $\alpha_{sk\sigma}$ denotes the proper unitary combination of lead operators which couple to the quantum dot and we dropped the part of the lead Hamiltonian which is decoupled from the dot. With the help of the definitions $V \equiv \sqrt{V_L^2 + V_R^2}$, $\alpha_{k\sigma} \equiv \alpha_{sk\sigma}$ and $\epsilon^*_{k\sigma} \equiv \frac{1}{2} (\epsilon_{Lk\sigma} + \epsilon_{Rk\sigma})$ the full Hamiltonian can be cast into a compact form

$$\hat{\mathcal{H}} = \sum_{k\sigma} \epsilon^*_{k\sigma} \alpha^\dagger_{k\sigma} \alpha_{k\sigma} + \sum_{k\sigma} V \left(d^\dagger_\sigma \alpha_{k\sigma} + \text{h.c.} \right) + \hat{\mathcal{H}}_d \,, \tag{4}$$

with $\hat{\mathcal{H}}_d$ as given in Eq. (1).

A. Ferromagnetic leads

For ferromagnetic materials electron-electron interaction in the leads give rise to magnetic order and spin-dependent DOS, $\rho_{r\uparrow}(\omega) \neq \rho_{r\downarrow}(\omega)$. Magnetic order of typical band ferromagnets like Fe, Co, and Ni is mainly related to electron correlation effects in the relatively narrow $3d$ sub-bands, which only weakly hybridize with $4s$ and $4p$ bands[20]. We can assume that due to a strong spatial confinement of d electron orbitals, the contribution of electrons from d sub-bands to transport across the tunnel barrier can be neglected[21]. In such a situation the system can be modeled by noninteracting[22] s electrons, which are spin polarized due to the exchange interaction with uncompensated magnetic moments of the completely localized d electrons. In mean-field approximation one can

model this exchange interaction as an effective molecular field, which removes spin degeneracy in the system of noninteracting conducting electrons, leading to a spin-dependent DOS.

Parallel and antiparallel leads' magnetization. – In experiments very frequently the electronic transport measurements are performed for two configurations of the leads' magnetization direction[10]: the parallel and antiparallel alignment. By comparison of electric current for these two configurations one can calculate the tunneling magnetoresistance (TMR) important parameter for the application of the magnetic tunnel junction[12].

In this paper we restrict the leads' magnetization direction to be either (i) *parallel*, i.e. the left and right lead have the DOS $\rho_{\mathrm{L}\sigma}(\omega)$ and $\rho_{\mathrm{R}\sigma}(\omega)$ respectively, so the total DOS corresponding to the total dispersion $\epsilon^*_{k\sigma}$ ($\forall k \in [-D_0; D_0]$) is given by $\rho_\sigma(\omega) = \rho_{\mathrm{L}\sigma}(\omega) + \rho_{\mathrm{R}\sigma}(\omega)$. (ii) *antiparallel*, the magnetization direction of one of the leads (let us consider the right one) is reverted so $\rho_{\mathrm{R}\sigma}(\omega) \to \rho_{\mathrm{R}\bar{\sigma}}(\omega)$, where $\bar{\sigma} = \downarrow$ ($\uparrow$) if $\sigma = \uparrow$ ($\downarrow$), so the total DOS is described then by $\rho_\sigma(\omega) = \rho_{\mathrm{L}\sigma}(\omega) + \rho_{\mathrm{R}\bar{\sigma}}(\omega)$. Here D_0 labels the full (generalized) bandwidth of the conduction band (further details can be found below). Effects related to leads with non-collinear leads' magnetization are not discussed here[23].

For the special case of both leads made of the same material in the parallel alignment $\rho_{\mathrm{L}\sigma}(\omega) = \rho_{\mathrm{R}\sigma}(\omega)$ and in the antiparallel alignment $\rho_{\mathrm{L}\sigma}(\omega) = \rho_{\mathrm{R}\bar{\sigma}}(\omega)$. Therefore for the antiparallel case it gives the total DOS to be spin independent $\rho_\uparrow(\omega) = \rho_{\mathrm{L}\uparrow}(\omega) + \rho_{\mathrm{R}\downarrow}(\omega) = \rho_{\mathrm{L}\downarrow}(\omega) + \rho_{\mathrm{R}\uparrow}(\omega) = \rho_\downarrow(\omega)$. In a such situation one can expect the usual Kondo effect as for normal (non-ferromagnetic) metallic leads, however, the conductance will be diminished due to mismatch of the density of states described by the prefactor of the integral in Eq. (23)

B. Different band structures

In this paper we will consider different type of total spin-dependent band structures $\rho_\sigma(\omega)$ independently of the particular magnetization direction of leads. The particular magnetization configuration will affect only the linear conductance G_σ due to the DOS mismatch for both leads as discussed in detail later.

1. Flat band

The simplest situation, where one can account spin asymmetry in is a flat band with the energy-independent DOS $\rho_\sigma(\omega) = \rho_\sigma$. Then the spin asymmetry can be parameterized just by single parameter the spin imbalance in the DOS at the Fermi energy $\omega = 0$. For flat bands the knowledge of the spin-polarization P of the leads, defined as

$$P = \frac{\rho_\uparrow(0) - \rho_\downarrow(0)}{\rho_\uparrow(0) + \rho_\downarrow(0)}\,, \tag{5}$$

equation is sufficient to fully parameterize $\rho_\sigma(\omega)$ (see Fig. 2). This particular DOS shape is a special due to the fact, that the particle-hole symmetry is conserved in the electrodes leading to particular behaviour for the symmetric Anderson model. This type model of the leads will be considered in Sec. V.

2. Stoner splitting

One can generalize this model and break the particle-hole symmetry by taking the Stoner splitting into account. A consequence of the conduction electron ferromagnetism is that the spin-dependent bands are shifted relative to each other (see Fig. 1). For a finite value of that shift Δ_σ, the spin-σ band ranges between $-D + \Delta_\sigma \le \omega \le D + \Delta_\sigma$ (with the 'original' bandwidth D). In the limit $\Delta_\sigma = 0$ only energies within the interval $[-D; D]$ are considered, a scheme usually used in the NRG calculations[7]. This relative shift between the two spin-dependent bands leads to so called Stoner splitting Δ, defined as

$$\Delta = \Delta_\downarrow - \Delta_\uparrow \tag{6}$$

at the band edges of the conduction band (see Fig. 10). The flat band model with a Stoner splitting and consequences of the particle-hole symmetry braking is considered in Sec. VI.

3. Arbitrary band structure

Since the spin-splitting of the dot level is determined by the coupling to all occupied and unoccupied (hole) electronic states in the leads, the shape of the whole band plays an important role. Therefore it is reasonable to consider arbitrary DOS shape, which cannot be parameterized by a particular set of parameters as the imbalance between $\uparrow$- and $\downarrow$-electrons at the Fermi energy or a Stoner splitting (see Fig. 1). Therefore in Sec. VII we will consider a model with a more complex band structure and in the next Sec. III we will develop the NRG technique for arbitrary band structure.

III. THE METHOD: NRG FOR ARBITRARY SPIN-DEPENDENT DENSITY OF STATES

In our analysis we take the ferromagnetic nature of the noninteracting leads by means of a *spin-* and *energy-dependent* DOS $\rho_\sigma(\omega)$ into account. A general example is given in Fig. 1. To compute the properties of the model described above we have extended numerical renormalization group (NRG) technique calculation to handle spin-dependent density of states. In order to understand to what extent the method applied here is different from the standard NRG it is adequate to briefly review the general concepts of NRG.

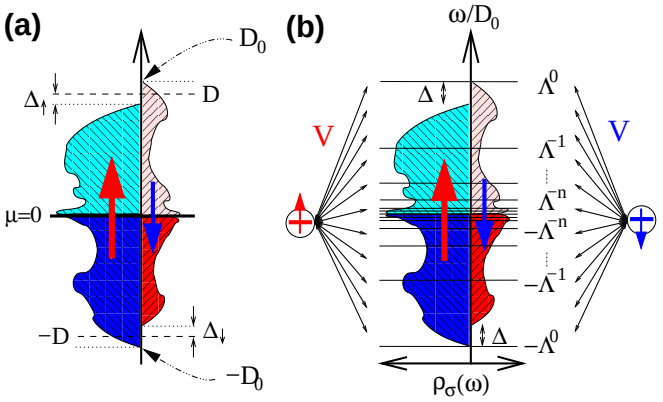

FIG. 1: (a) Example of an *energy*- and *spin*-dependent leads DOS $\rho_\sigma(\omega)$ with an additional spin-dependent shift Δ_σ. To perform the logarithmic discretization a generalized bandwidth D_0 is defined. Since we allow for bands with energy and spin dependence the discretization is performed for each spin-component separately, see panel (b). Since $\hat{\mathcal{H}}_{\ell d}$ does not include spin-flip processes an impurity electron of spin σ [circles in panel (b)] couples to lead electrons of spin σ, $\sigma =\uparrow$ ($\downarrow$), only. Panel (b) also illustrates that impurity electrons couple to leads' electron and hole sates with *arbitrary* energy ω, $|\omega| \leq D_0$.

The NRG technique was invented by Wilson in the 70's to solve the Kondo problem[14] – later it was extended to handle other quantum impurity models as well[24–26,28]. In his original work Wilson considered a spin-independent flat density of states for the conduction electrons. Closely following Refs[17,27] –where the mapping for the case of energy-dependent DOS was given– we generalize that procedure for the case of the Hamiltonian given in Eq. (4) which contains leads with an *energy*- and *spin*-dependent DOS.

It is convenient to bring the Hamiltonian given by Eq. (4), into a continuous representation[27] before the generalized mapping is started. The replacement of the discrete fermionic operators by continuous ones, $\alpha_{k\sigma} \rightarrow \alpha_{\omega\sigma}$, translates the lead and the tunneling part of the Hamiltonian into

$$\hat{\mathcal{H}}_\ell = \sum_\sigma \int_{-1}^{1} d\omega \; g_\sigma(\omega) \; \alpha^\dagger_{\omega\sigma}\alpha_{\omega\sigma} \tag{7}$$

$$\hat{\mathcal{H}}_{\ell d} = \sum_\sigma \int_{-1}^{1} d\omega \; h_\sigma(\omega) \; \left(d^\dagger_\sigma \alpha_{\omega\sigma} + \text{h.c.}\right) . \tag{8}$$

As shown in Ref. 27 the hereby defined generalized *dispersion* $g_\sigma(\omega)$ and *hybridization* $h_\sigma(\omega)$ functions have to satisfy the relation

$$\frac{\partial g_\sigma^{-1}(\omega)}{\partial \omega} \left[h_\sigma\left(g_\sigma^{-1}(\omega)\right)\right]^2 = \rho_\sigma(\omega)\left[V_\sigma(\omega)\right]^2 , \tag{9}$$

where $g_\sigma^{-1}(\omega)$ is the inverse of $g_\sigma(\omega)$, what ensures that the action on the impurity site is identical both in the discrete and the continuous representation. Note that there are many possibilities to satisfy Eq. (9).

The key idea of Wilson's NRG [14] is a logarithmic discretization of the conduction band, by introducing a discretization parameter Λ, which defines energy intervals $]-D_0\Lambda^{-n}; -D_0\Lambda^{-n-1}]$ and $[D_0\Lambda^{-n-1}; D_0\Lambda^{-n}[$ in the conduction band ($n \in \mathbf{N}_0$). Within the n-th interval of width $d_n = \Lambda^{-n}\left(1-\Lambda^{-1}\right)$ a Fourier expansion of the lead operators $\Psi^\pm_{np}(\omega)$ with fundamental frequency $\Omega_n = 2\pi/d_n$ is defined

$$\Psi^\pm_{np}(\omega) = \begin{cases} \frac{1}{\sqrt{d_n}} e^{\pm i\Omega_n p\omega} & \text{if } \Lambda^{-(n+1)} \leq \pm\omega < \Lambda^{-n} \\ 0 & \text{else} \end{cases}$$

Here the subscripts n and p ($\in \mathbf{Z}$) label the corresponding interval and the harmonic index, respectively, while the superscript marks positive (+) or negative (−) intervals, respectively.

The above defined Fourier series now allows one to replace the continuous fermionic conduction band operators $a_{\omega\sigma}$ by discrete ones $a_{np\sigma}$ ($b_{np\sigma}$) of harmonic index p and spin σ acting on the n-th positive (negative) interval only

$$\alpha_{\omega\sigma} = \left\{ \sum_{np} \left[a_{np\sigma}\Psi^+_{np}(\omega) + b_{np\sigma}\Psi^-_{np}(\omega)\right] \right\}. \tag{10}$$

Impurity electrons couple *only* to the $p = 0$ mode of the lead operators, given the energy-dependent generalized hybridization $h_\sigma(\omega)$ is replaced by a constant hybridization, $h_\sigma(\omega) \rightarrow h^+_{n\sigma}$ for $\omega > 0$ (or $h^-_{n\sigma}$ for $\omega < 0$, respectively). Obviously, the particular choice of constant hybridization $h^\pm_{n\sigma}$ demands the generalized dispersion $g_\sigma(\omega)$ to be adjusted accordingly, such that Eq. (9) remains valid. Details of this procedure can be found in Appendix A. Since we adopt this strategy the harmonic index p (the impurity couples only to lead operators of harmonic index $p = 0$) will be dropped below.

Defining a fermionic operator

$$f_{0\sigma} \equiv \frac{1}{\sqrt{\xi_{0\sigma}}} \sum_n \left(a_{n\sigma}\gamma^+_{n\sigma} + b_{n\sigma}\gamma^-_{n\sigma}\right), \tag{11}$$

with $\xi_{0\sigma} = \sum_n \left[\left(\gamma^+_{n\sigma}\right)^2 + \left(\gamma^-_{n\sigma}\right)^2\right] = \int_{-1}^{1} \Gamma_\sigma(\omega)d\omega$ and the coefficients $\gamma^\pm_{n\sigma}$ as given in Appendix A[29], reveals that the impurity effectively couples to a *single* fermionic degree of freedom only, the zeroth site of the Wilson chain [for further details see Eq. (A2)]. Therefore the tunneling part of $\hat{\mathcal{H}}$ can be written in a compact form as

$$\hat{\mathcal{H}}_{\ell d} = \sum_\sigma \left[\sqrt{\frac{\xi_{0\sigma}}{\pi}} \left(d^\dagger_\sigma f_{0\sigma} + \text{h.c.}\right)\right]. \tag{12}$$

The final step in the NRG-procedure is the transformation of the conduction band $\hat{\mathcal{H}}_\ell$ into the form of a linear chain. This goal is achieved via the tridiagonalization procedure developed by Lánczos[30]

$$\hat{\mathcal{H}}_\ell = \sum_{\sigma n=0}^{\infty} \left[\varepsilon_{n\sigma} f^\dagger_{n\sigma} f_{n\sigma} + t_{n\sigma}\left(f^\dagger_{n\sigma} f_{n+1\sigma} + f^\dagger_{n+1\sigma} f_{n\sigma}\right)\right]. \tag{13}$$

In general the on-site energies $\varepsilon_{n\sigma}$ and hopping matrix elements $t_{n\sigma}$ along the Wilson-chain need to be determined numerically. Besides the matrix elements $\epsilon_{n\sigma}$ and $t_{n\sigma}$ coefficients $u_{nm\sigma}$ and $v_{nm\sigma}$, which define the fermionic operators $f_{n\sigma}$

$$f_{n\sigma} \equiv \sum_{m=0}^{\infty} \left(u_{nm\sigma} a_{m\sigma} + v_{nm\sigma} b_{m\sigma} \right) \tag{14}$$

already used in Eq. (13), need to be determined. One immediately anticipates from Eq. (11)

$$u_{0m\sigma} = \gamma^{+}_{m\sigma} / \sqrt{\xi_{0\sigma}} \ , \quad v_{0m\sigma} = \gamma^{-}_{m\sigma} / \sqrt{\xi_{0\sigma}} \ . \tag{15}$$

Equations which determine the matrix elements $\epsilon_{n\sigma}$ and $t_{n\sigma}$ and the coefficients $u_{nm\sigma}$ and $v_{nm\sigma}$ are given in Appendix B. Note that the on-site energies $\varepsilon_{n\sigma}$ vanish in the presence of particle-hole symmetry in the leads.

To summarize: Hamiltonians as the one given in Eq. (4) can be cast into the form of a linear chain $\hat{\mathcal{H}}_{\rm LC}$

$$\begin{aligned} \hat{\mathcal{H}}_{\rm LC} \ &= \hat{\mathcal{H}}_d + \sqrt{\xi_{0\sigma}/\pi} \sum_{\sigma} [d^{\dagger}_{\sigma} f_{0\sigma} + f^{\dagger}_{0\sigma} d_{\sigma}] \\ &+ \quad \sum_{\sigma n=0}^{\infty} [\varepsilon_{n\sigma} f^{\dagger}_{n\sigma} f_{n\sigma} + t_{n\sigma} (f^{\dagger}_{n\sigma} f_{n+1\sigma} + f^{\dagger}_{n+1\sigma} f_{n\sigma})] \ , \end{aligned} \tag{16}$$

even though one is dealing with energy and spin-dependent leads. In general, however, this involves numerical determination of the matrix elements $\varepsilon_{n\sigma}$ and $t_{n\sigma}$ [17] in contrast to Krishna-murthy[24] *et al.* (who considered flat bands) no closed analytical expression for those matrix elements is known.

Eq. (16) nicely illustrates the strength of the NRG-procedure: As a consequence of the energy separation guaranteed by the logarithmic discretization, the hopping rate along the chain decreases as $t_n \sim \Lambda^{-n/2}$ (the on-site energies decays even faster) which allows us to diagonalize the chain Hamiltonian iteratively and in every iteration to keep the states with the lowest lying energy eigenvalues as the most relevant ones. This very fact underlines that this method does not rely on any assumptions concerning leading order divergences.[31]

IV. PERTURBATIVE SCALING ANALYSIS

We can understand the spin-splitting of the spectral function using Haldane's scaling approach[16], where quantum charge fluctuations are integrated out. The behavior discussed in this paper can be explained as an effect of spin-dependent quantum charge fluctuations, which lead to a spin-dependent renormalization of the dot's level position $\tilde{\epsilon}_{{\rm d}\sigma}$ and a spin-dependent level broadening Γ_σ, which in turn induce spin splitting of the dot level and the Kondo resonance. Within this approach a spin-splitting of the local dot level, $\Delta\epsilon_{\rm d} \equiv \delta\epsilon_{{\rm d}\uparrow} - \delta\epsilon_{{\rm d}\downarrow} + B$, which depends on the *full* band structure of the leads is obtained[13]

where

$$\delta\epsilon_{{\rm d}\sigma} \simeq -\frac{1}{\pi} \int d\omega \left\{ \frac{\Gamma_\sigma(\omega)[1-f(\omega)]}{\omega - \epsilon_{{\rm d}\sigma}} + \frac{\Gamma_{\bar{\sigma}}(\omega) f(\omega)}{\epsilon_{{\rm d}\bar{\sigma}} + U - \omega} \right\} \tag{17}$$

Note that the splitting is *not* only determined by the leads spin polarization P, i. e. the splitting is not only a property of the Fermi surface. Eq. (17) is the key equation to explain the physics of the (spin-dependent) splitting of the local level $\epsilon_{{\rm d}\sigma}$. This equation explains the spin-dependent occupation and consequently the splitting of the spectral function of a dot that is contacted to leads with a particular band-structure. The first term in the curly brackets corresponds to electron-like processes, namely charge fluctuations between a single occupied state $|\sigma\rangle$ and the empty $|0\rangle$ one, and the second term to hole-like processes, namely charge fluctuations between the states $|\sigma\rangle$ and $|2\rangle$. The amplitude of the charge fluctuations is proportional to Γ, which for $\Gamma \gg T$ determines the width of dot levels observed in transport.

The exchange field given by Eq. (17) gives rise to precession of an accumulated spin on the quantum dot attached to leads with non-collinear leads' magnetization are not discussed here[23].

A. Flat band

Eq. (17) predicts that even for systems with spin-asymmetric bands $\rho_\uparrow(\omega) \neq \rho_\downarrow(\omega)$, the integral can give $\Delta\epsilon = 0$, which corresponds to a situation where the renormalization of $\epsilon_{{\rm d}\sigma}$ due to electron-like processes are compensated by hole-like processes. An example is a system consisting of particle-hole symmetric bands, $\rho_\sigma(\omega) = \rho_\sigma(-\omega)$, where no splitting of the Kondo resonance ($\Delta\epsilon_{\rm d} = 0$) for the symmetric point, $\epsilon_{\rm d} = -U/2$, appears.

For a flat band $\rho_\sigma(\omega) = \rho_\sigma$, Eq. (17) can be integrated analytically. For $D_0 \gg U$, $|\epsilon_{\rm d}|$ one finds: $\Delta\epsilon \simeq (P\,\Gamma/\pi)\,{\rm Re}[\phi(\epsilon_{\rm d}) - \phi(U+\epsilon_{\rm d})]$, where $\phi(x) \equiv \Psi(\frac{1}{2} + ix/2\pi T)$ and $\Psi(x)$ denotes the digamma function. For $T = 0$, the spin-splitting is given by

$$\Delta\epsilon_{\rm d} \simeq \frac{P\,\Gamma}{\pi} \ln\left(\frac{|\epsilon_{\rm d}|}{|U+\epsilon_{\rm d}|} \right) \ , \tag{18}$$

showing a logarithmic divergence for $\epsilon_{\rm d} \to 0$ or $U + \epsilon_{\rm d} \to 0$.

B. Stoner splitting

For real systems p-h symmetric bands cannot be assumed, however the compensation $\Delta\epsilon = 0$ using a proper tuning of the gate voltage $\epsilon_{\rm d}$ is still possible. We can analyze also the effect of the Stoner splitting by considering a flat-band structure in Fig. 2 using the value of the Stoner splitting $\Delta = 0.2(\frac{D}{D_0})D_0$. Then also from Eq. (17) we can expect an additional spin-splitting of the dot level

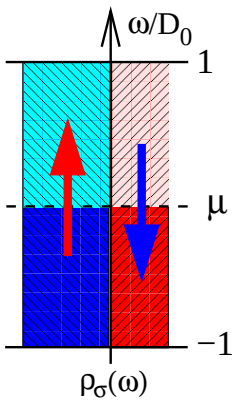

FIG. 2: The leads density of states of a flat $[\rho_s(\omega) = \rho_\sigma]$ but spin-dependent ($\rho_\uparrow \neq \rho_\downarrow$) band for spin polarization $P = 0.2$. The dark region marks the filled states below the Fermi energy. Since $\Delta_\uparrow = \Delta_\downarrow = 0$ the generalized bandwidth $D_0 = D$.

induced by the presence of the Stoner field in the leads even for spin polarization $P = 0$ given by

$$\Delta\epsilon_{\rm d}^{\rm (St)} \simeq \frac{\Gamma}{2\pi} \ln\left[\frac{(-\epsilon_{\rm d} + D_0 - \Delta)(U + \epsilon_{\rm d} + D_0 - \Delta)}{(-\epsilon_{\rm d} + D_0)(U + \epsilon_{\rm d} + D_0)}\right] \quad (19)$$

which for the symmetric level position, $\epsilon_{\rm d} = -U/2$, it leads to

$$\Delta\epsilon_{\rm d}^{\rm (St)} \simeq \frac{\Gamma}{\pi} \ln\left[\frac{U/2 + \epsilon_{\rm d} + D_0 - \Delta}{U/2 + \epsilon_{\rm d} + D_0}\right] , \quad (20)$$

Eq. (19) also shows that the characteristic energy scale of the spin-splitting is given by Γ rather than by the Stoner splitting Δ ($\Delta \gg \Gamma$), since the states far from the Fermi surface enter Eq. (17) only with a logarithmic weight. The difference can be as large as three orders of the magnitude, so in metallic ferromagnet the Stoner splitting energy is of the order $\Delta \sim 1\ eV$ but still the effective molecular filed $\Delta\epsilon_{\rm d}^{\rm (St)}$ generated by it is a small fraction of Γ - of order of $1\ meV$ so comparable with the Kondo energy scale for molecular single-electron transistors.[10] However, the Stoner splitting introduces a strong p-h asymmetry, so it can influence the character of gate voltage dependence significantly.

In the next Section we analyze the effect of different type of the band structure using numerical renormalization group technique and compare it to that obtained in this Section by scaling procedure.

V. FLAT BANDS WITHOUT STONER SPLITTING

We start our analysis by considering normalized flat bands without the Stoner splitting (i. e. $D_0 = D$), as sketched in Fig. 2, with finite spin-polarization $P \neq 0$ [defined via Eq. (5)].[32] In this particular case – of spin- (but not energy-) dependent coupling $\Gamma_\sigma \equiv \pi\rho_\sigma V^2$ – the

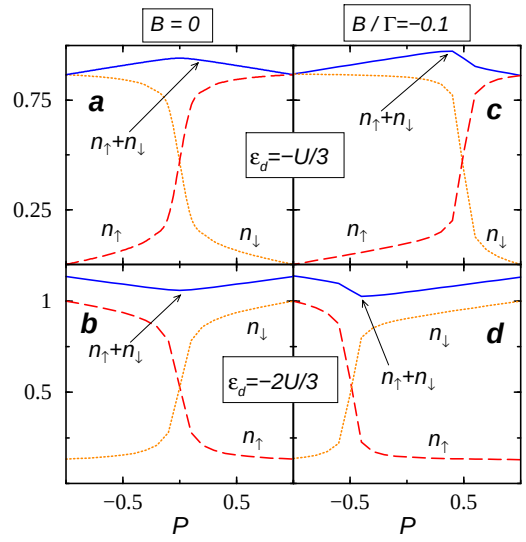

FIG. 3: (a)-(d): Spin-dependent occupation n_σ of the local level as a function of the leads' spin polarization P for $\epsilon_d = -U/3$ [(a) and (c)] and $\epsilon_d = -2U/3$ [(b) and (d)](related by the particle-hole symmetry) for $B = 0$ (left column) and $B = -0.1\ \Gamma$ (right column). For finite spin-polarization $P \neq 0$ the condition $n_\uparrow = n_\downarrow$ can only be obtained by an appropriately tuned magnetic field, as shown in (c) and (d). Parameters: $U = 0.12\ D_0$, $\Gamma = U/6$.

coupling Γ_σ can be parametrized via P, $\Gamma_{\uparrow(\downarrow)} = \frac{1}{2}\Gamma(1 \pm P)$ [here $+$ $(-)$ corresponds to spin $\uparrow$ $(\downarrow)$], where $\Gamma = \Gamma_\uparrow + \Gamma_\downarrow$. Leads with a DOS as the one analyzed in this section have for instance been studied in Ref.[7,8].

Since $\Gamma_\sigma \equiv \pi\rho_\sigma V^2$ the spin-dependence of Γ_σ can be absorbed by replacing $V \to V_\sigma = V\sqrt{\frac{1}{2}(1 \pm P)}$ in Eq. (4), i. e. a spin-dependent *hopping* matrix element, while treating the leads as unpolarized ones ($\rho_\sigma \to \rho$). This procedure has the particular advantage that the 'standard' NRG procedure[24] can be applied meaning that the on-site energies (tunneling matrix elements), defined in Eq. (13), along the Wilson chain $\varepsilon_{n\sigma}$ vanish, while $t_{n\sigma}$'s turn out to be *spin-independent*. Therefore it does not involve the solution of the tedious equations given in Appendix B.

A. Spin and charge state

Consequently we start our numerical analysis by computing the spin-resolved dot occupation $n_\sigma \equiv \langle \bar{n}_\sigma \rangle$, which is a static property. Fig. 3 shows the spin-resolved impurity occupation as a function of the spin-polarization P of the leads. Fig. 3(a) and (c) corresponds to a gate-voltage of $\epsilon_{\rm d} = -U/3$ (where the total occupation of the system $n_\uparrow + n_\downarrow < 1$) whereas the second line to $\epsilon_{\rm d} = -2U/3$ (with $n_\uparrow + n_\downarrow > 1$). The total occupation of the system $n_\uparrow + n_\downarrow$ decreases (increases) for $\epsilon_{\rm d} = -U/3$ ($\epsilon_{\rm d} = -2U/3$) when the spin-polarization of the leads is finite $P \neq 0$. Note

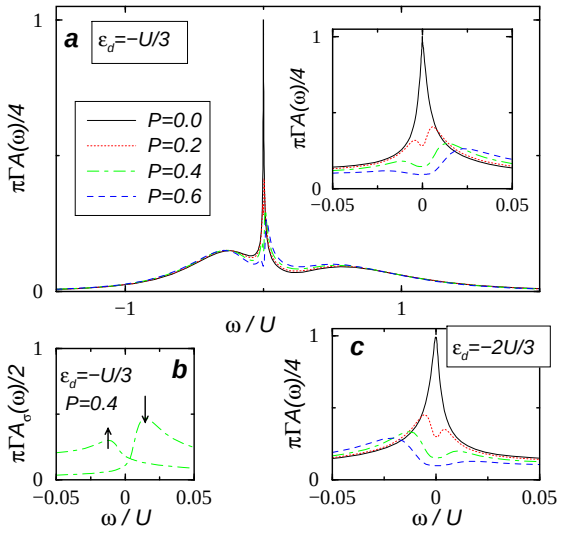

FIG. 4: Total spectral functions $A(\omega) = \sum_\sigma A_\sigma(\omega)$ for various values of the spin polarization P. (a) For $\epsilon_{\rm d} = -U/3$ an increase in P results in a splitting and suppression of the Kondo resonance (see inset). The effect of finite P on the Hubbard peaks is less significant. The spin-resolved spectral function $A_\sigma(\omega)$, shown in (b), reveals that $A_\uparrow(\omega)$ and $A_\downarrow(\omega)$ differ significantly from each other for $P \neq 0$. (c) Spectral function for the same values of P as in (a) but for $\epsilon_d = -2/3U$ [due to particle-hole symmetry the results are mirrored as compare to (a), however with inverted spins]. Parameters: $U = 0.12D_0$, $B = 0$, $\Gamma = U/6$.

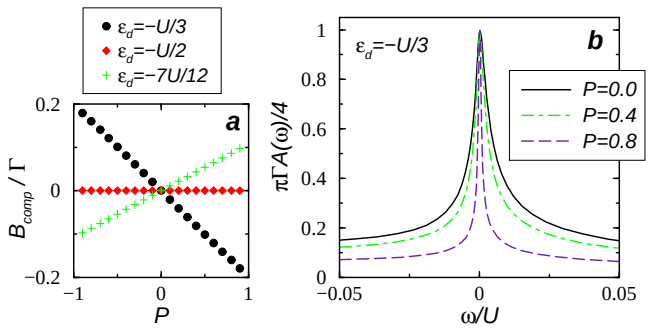

FIG. 5: (a) Compensation field $B_{\rm comp}(P)$ for different values of ϵ_d. For flat bands $B_{\rm comp}$ depends linearly on the leads polarization. At the point where there is particle-hole symmetry, so for gate voltage ($\epsilon_d = -U/2$), $B_{\rm comp}(P) = 0$ for any value of P, i. e. the spectral function is not split for any value of P even though $B = 0$. (b) Spectral function for various values of P for $B = B_{\rm comp}$. Note the sharper resonance in the spectral function, i. e. a reduced Kondo temperature $T_{\rm K}$.

that both situations, $\epsilon_{\rm d} = -U/3$ and $\epsilon_{\rm d} = -2U/3$), are symmetric in respect of changing particle into hole states and vice versa, which is possible only for the leads with particle-hole symmetry. For the gate voltage $\epsilon_{\rm d} = -U/2$ there is a particle-hole symmetry in the whole system leads with a DOS which does share this symmetry even in the presence of spin asymmetry. Note, whereas a finite spin polarization leads to a decrease in $n_\uparrow + n_\downarrow$ for $\epsilon_{\rm d} > -U/2$, cf. Fig. 3(a), it results in an increase in $n_\uparrow + n_\downarrow$ for $\epsilon_{\rm d} < -U/2$, cf. Fig. 3(b). Obviously, for $P = 0$ and in absence of an external magnetic field the impurity does not have a preferred occupation $n_\uparrow = n_\downarrow$. Any finite value of P violates this relation: $n_\uparrow > n_\downarrow$ for $P > 0$ and $\epsilon_{\rm d} > -U/2$ (since $\delta\epsilon_{{\rm d}\uparrow} \sim \Gamma_\downarrow < \Gamma_\uparrow \sim \delta\epsilon_{{\rm d}\downarrow}$). For $\epsilon_{\rm d} < -U/2$, on the other hand, the opposite behavior is found.

The effect on the impurity of a finite leads polarization, namely to prefer a certain spin species, can be compensated by a locally applied magnetic field, as shown in Figs. 3(c) and (d). For $\epsilon = -U/3$ and $B/\Gamma = -0.1$, cf. Fig. 3(c), the impurity is *not* occupied by a preferred spin species, $n_\uparrow = n_\downarrow$, for $P \sim 0.5$. Due to particle-hole symmetry the same magnetic field absorbs a lead polarization of $P \sim -0.5$ for $\epsilon = -2U/3$, cf. Fig. 3(d). The magnetic field which restores the condition $n_\uparrow = n_\downarrow$, henceforth denote as compensation field $B_{\rm comp}(P)$, will be of particular interest below.

B. Single-particle spectral function

Using the NRG technique we can access to the spin-resolved single-particle spectral density $A_\sigma(\omega, T, B, P) = -\frac{1}{\pi}{\rm Im}\mathcal{G}^R_{d,\sigma}(\omega)$ for arbitrary temperature T, magnetic field B, and spin polarization P, where $G^R_\sigma(\omega)$ denotes a retarded Green function. We can relate the asymmetry in the occupancy, $n_\uparrow \neq n_\downarrow$, to the occurrence of charge fluctuations in the dot and broadening and shifts the position of the energy levels (for both spin up and down). For $P \neq 0$, the charge fluctuations and hence level shifts and level occupations become *spin-dependent*, causing the dot level to split[6] and the dot magnetization $n_\uparrow - n_\downarrow$ to be finite. As a result, the Kondo resonance is also spin-split and suppressed Fig. 4(b), similarly to the effect of an applied magnetic field[33]. This means that Kondo correlations are reduced or even completely suppressed in the presence of ferromagnetic leads.

Note the asymmetry in the spectral function for $P \neq 0$ which stems from the spin-dependent hybridization Γ_σ. In Fig. 4(b), where the spin-resolved spectral function is plot, reveals the origin of the asymmetry around the Fermi energy of the spectral function. The spectral function obtained for polarized leads has to be contrasted to that of a dot asserted to a local magnetic field, where a nearly *symmetric* (perfect symmetry is only for the symmetric Anderson model) suppression and splitting of the Kondo resonance (around the Fermi energy) appears.[33] In Fig. 4(c) the gate voltage ($\epsilon_{\rm d} = -2U/3$) is chosen such that it is particle-hole symmetric to the case shown in Fig. 4(a). Due to the opposite particle-hole symmetry, the obtained spectral function in Fig. 4(c) is nothing else but the spectral function shown in Fig. 4(a) mirrored around the Fermi energy.

Fig. 3(c) and (d) showed that a finite magnetic field B can be used to recover the condition $n_\uparrow = n_\downarrow$. Indeed, for

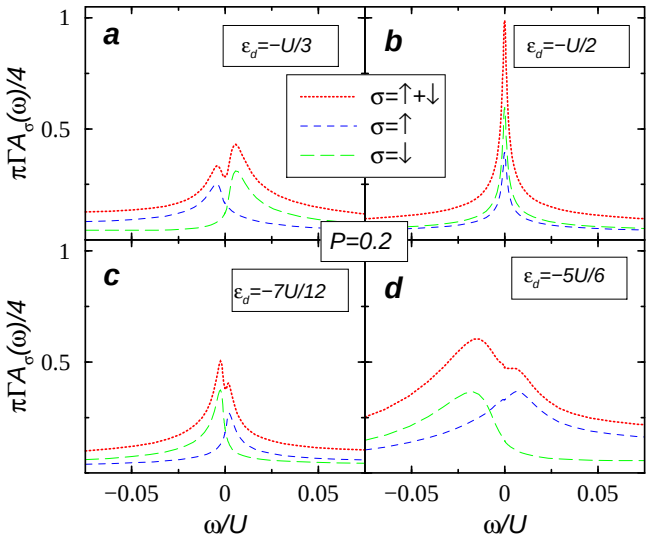

FIG. 6: Spin-dependent spectral function $A_\sigma(\omega)$ for various values of $\epsilon_{\rm d}$, fixed $P = 0.2$, and $B = 0$ [(blue) dashed: $A_\uparrow(\omega)$, (green) long-dashed: $A_\uparrow(\omega)$ and (red) dotted $A(\omega) = \sum_\sigma A_\sigma(\omega)$]. The splitting between $A_\uparrow$ and $A_\downarrow$ changes its sign at $\epsilon_{\rm d} = -U/2$. The spectral function $A(\omega)$ is plot for several values of P for $\epsilon_{\rm d} = -U/3$ in Fig. 4 (a). The splitting of the spectral function $A(\omega)$ depends as well on $\epsilon_{\rm d}$ as on P. Parameters: $U = 0.12D_0$, $\Gamma = U/6$.

any lead polarization P a *compensation* field $B_{\rm comp}(P)$ exists at which the impurity is not preferably occupied by a particular spin species. To a good approximation $B_{\rm comp}(P)$ has to be chosen such that the induced spin-splitting of the local level is compensated[37]. One consequently expects a linear P-dependence of $B_{\rm comp}$ from Eq. (18). Fig.5(a) shows the P-dependence of $B_{\rm comp}$ for various values of $\epsilon_{\rm d}$ obtained via NRG. The numerically found behavior can be explained through Eq. (18). It confirms that the slope of $B_{\rm comp}$ is negative (positive) for $\epsilon_{\rm d} > -U/2$ ($\epsilon_{\rm d} < -U/2$) and that $B_{\rm comp}(P) = 0$ for $\epsilon_{\rm d} = -U/2$.

The fact that this occurs simultaneously with the disappearance of the Kondo resonance splitting suggests that the local spin is fully screened at $B_{\rm comp}$. The expectation of an unsplit Kondo resonance in presence of the magnetic field $B_{\rm comp}$ is nicely confirmed by our numerics in Fig. 5(b) for $\epsilon_{\rm d} = -U/3$. Moreover, the sharpening of the Kondo resonance in the spectral function upon an increase in P (indicating a decrease in the Kondo temperature $T_{\rm K}$) can be extracted from this plot. The associated binding energy of the singlet (the Kondo temperature $T_{\rm K}$) is consequently reduced.

Having demonstrated that the Kondo resonance can be fully recovered for $B_{\rm comp}$ even though $P \neq 0$ we show that there is also the possibility to recover the unsplit Kondo resonance via an appropriately tuned gate-voltage. In Fig. 6 we plot the spin-resolved spectral function for various values of $\epsilon_{\rm d}$ for $P = 0.2$ and $B = 0$. Note that one can easily identify whether the Kondo resonance is fully recovered from the positions of $A_\sigma(\omega)$ relative to each other. Since a dip in the total spectral function $A(\omega) = \sum_\sigma A_\sigma(\omega)$ is not present for a modest shift of $A_\sigma(\omega)$ w. r. t. each other, we identify an unsplit Kondo resonance with perfectly aligned spin-resolved spectral functions henceforth.

Clearly one can identify from Fig. 6 that the spectral function is split for any value $\epsilon_{\rm d} \neq -U/2$. This splitting changes its sign at $\epsilon_{\rm d} = -U/2$. For the particular case $\epsilon_{\rm d} = -U/2$, cf. Fig. 6(b), the spectral function reaches the unitary limit. For this gate voltage the spin-resolved spectral functions $A_\sigma(\omega)$ have a different height as predicted from the Friedel sum rule Eq. (21).

C. Friedel sum rule

A direct consequence of the spin-splitting of the local level and the accompanied $n_\uparrow \neq n_\downarrow$ for $P \neq 0$ and $B = 0$ can be explained by means of the Friedel sum rule,[34] an exact $T = 0$ relation valid also for arbitrary values of P and B. This formula relates the height of the spectral function (at the Fermi energy) and the phase shift of the electrons scattered by the impurity. As already pointed out spin-polarized electrodes induce a splitting the local impurity level resulting in a spin-dependent occupation of the impurity. Thus the knowledge of the local occupation can be used to anticipate (via the Friedel sum rule) that the local spectral function becomes spin-split and suppressed (similar to the presence of a local magnetic field) in the presence of spin-polarized leads.

According to Friedel sum rule, the height of the spectral function at the Fermi energy $A_\sigma(0)$ are fully determined by the level occupation n_σ

$$\phi_\sigma = \pi n_\sigma, \qquad A_\sigma(0) \;=\; \frac{\sin^2(\pi n_\sigma)}{\pi\Gamma_\sigma}\,, \qquad (21)$$

where ϕ_σ being the spin dependent phase shift. This implies a split and suppressed Kondo resonance for $P \neq 0$ in absence of a magnetic field.

An equal spin occupation, $n_\uparrow = n_\downarrow$, can be obtained only for an appropriate external magnetic field $B = B_{\rm comp}$. For the latter, in the local moment regime ($n \approx 1$) we have $n_\uparrow = n_\downarrow \approx 0.5$, so that $\phi_\uparrow = \phi_\downarrow \approx \pi/2$, which implies that the peaks of $A_\uparrow$ and $A_\downarrow$ are aligned. Thus, the Friedel sum rule clarifies why the magnetic field $B_{\rm comp}$ at which the splitting of the Kondo resonance disappears, coincides with that for which $n_\uparrow = n_\downarrow$. Eq. (21) indicates a new feature namely that the amplitude of the Kondo resonance becomes spin dependent (see also the discussion in Sec. V E).

It is important to point out that Eq. (21) is valid only for the leads with particle-hole symmetry (see Ref.35). For arbitrary DOS shape it is possible to generalize the Friedel sum rule.

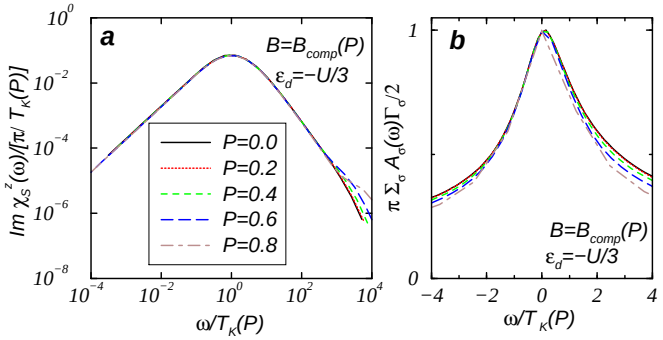

FIG. 7: The isotropic Kondo effect, accompanied by universal scaling, can be recovered even for $P \neq 0$ and $B = B_{\rm comp}$ since both the spin-susceptibility $\mathrm{Im}\chi_S^z$ (a) and the spectral function (b) collapse onto a universal curve. This statement holds for any value of ϵ_d with some corresponding compensation fields as given in Fig. 5(a). Parameters: $U = 0.12D_0$, $\epsilon_d = -U/3$, $\Gamma = U/6$.

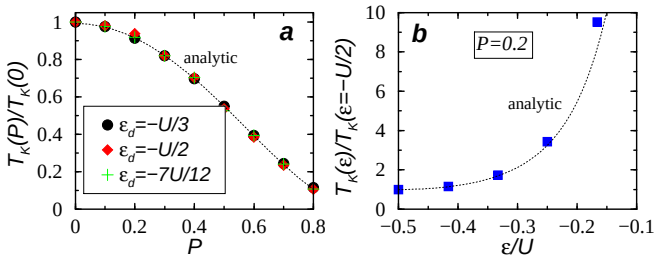

FIG. 8: (a) Spin polarization dependence of the Kondo temperature $T_{\rm K}(P)$ [obtained by applying an appropriate $B = B_{\rm comp}(P, \epsilon_{\rm d})$]. The functional dependence of $T_{\rm K}(P)$ found via a poor man's scaling analysis (dotted line), see Eq.(6) of Ref. 6, is confirmed by the NRG analysis. The plot confirms that a dot tuned to the local moment regime, $\sum_\sigma n_\sigma \simeq 1$, shows the universal P-dependence of $T_{\rm K}(P)$, for arbitrary values of $\epsilon_{\rm d}$. (b) The $\epsilon_{\rm d}$-dependence of $T_{\rm K}$ for fixed $P = 0.2$ at $B = B_{\rm comp}$. As long as the impurity remains in the local moment regime Haldane's formula[16] for $T_{\rm K}$ (dotted line) properly describes $T_{\rm K}(\epsilon_{\rm d})$ even though the leads have a finite spin polarization. Parameters: $U = 0.12\ D_0$, $\Gamma = U/6$.

D. Spin-spectral function - Kondo temperature

We already stated above that the Kondo temperature $T_{\rm K}$ decreases when the leads polarization P is increased. Obviously, $T_{\rm K}$ has to vanish when we are dealing with fully spin-polarized leads $|P| = 1$. To obtain $T_{\rm K}(P)$ we calculated the imaginary part of the quantum dot spin spectral function

$$\chi_S^z(\omega) = \mathcal{F}\{i\Theta(t)\langle[S_z(t), S_z(0)]\rangle\} \qquad (22)$$

($\mathcal{F}$ denotes the Fourier transform), see also Fig. 7(a), in presence of the appropriate $B_{\rm comp}(P, \epsilon_{\rm d})$ and identified the maximum in $\mathrm{Im}\chi_S^z$ with $T_{\rm K}(P)$. Fig. 8(a) shows $T_{\rm K}(P)$ normalized to $T_{\rm K}(P = 0)$ for different values of $\epsilon_{\rm d}$. As shown in Ref.[6,7] the functional dependence of $T_{\rm K}(P)$ can be nicely explained within the framework of poor man's scaling. Note that the decrease in $T_{\rm K}$ is rather weak for a modest value of P. In Fig. 7(b) we plot, additionally to $T_{\rm K}(P)$, the gate-voltage dependence of $T_{\rm K}(\epsilon_{\rm d})$ normalized to $T_{\rm K}(\epsilon_{\rm d} = -U/2)$ (where the Kondo temperature is minimal) for fixed $P = 0.2$. In presence of $B_{\rm comp}(P, \epsilon_{\rm d})$ this functional dependence of the Kondo temperature can analytically be described via Haldane's formula[16] for the Kondo temperature of a single level dot coupled to unpolarized leads, $T_{\rm K} = \frac{1}{2}\sqrt{U\Gamma}e^{\pi\epsilon_d(\epsilon_d+U)/\Gamma U}$. This fact is another manifestation that indeed the usual Kondo effect can be recovered in presence of spin-polarized leads, given the appropriate $B_{\rm comp}(P, \epsilon_{\rm d})$ is applied.

Having shown that the coexistence of spin-polarization in the leads and the Kondo effect is possible (given a magnetic field B is tuned appropriately at a given gate-voltage $\epsilon_{\rm d}$), we plot the properly rescaled spin-susceptibility $\mathrm{Im}\chi_S^z$, see Fig. 7(a), and spectral function, see Fig. 7(b), confirming that the isotropic Kondo effect is recovered. The expected collapse of $\mathrm{Im}\chi_S^z$ and $\sum_\sigma \Gamma_\sigma A_\sigma(\omega)$ onto a universal curve for temperatures below $T_{\rm K}$ [note that $T_{\rm K}$ depends on P, see e. g. Fig. 5(b)] is confirmed by our numerical results. For energies much bigger that $T_{\rm K}$, $\omega \gg T_{\rm K}$, universal scaling is lost and the curves start to deviate from each other.

E. Conductance

The knowledge of the spectral function enables us to compute quantities which are experimentally accessible, such as the linear conductance. To investigate the question whether spin-polarized ferromagnetic leads introduce a spin-dependent current we compute the spin-resolved conductance G_σ,

$$G_\sigma = \frac{e^2}{\hbar}\frac{2\Gamma_{{\rm L}\sigma}\Gamma_{{\rm R}\sigma}}{(\Gamma_{{\rm L}\sigma}+\Gamma_{{\rm R}\sigma})}\int_{-\infty}^{\infty} d\omega A_\sigma(\omega)\left(-\frac{\partial f(\omega)}{\partial\omega}\right) \qquad (23)$$

with $f(\omega)$ denoting the Fermi function (remember that we choose $\Gamma_{{\rm L}\sigma} = \Gamma_{{\rm R}\sigma}$). The total conductance G is nothing else but the sum of the spin-resolved conductances $G = \sum_\sigma G_\sigma$. Based on the Friedel sum rule, Eq. (21), we expect the height of the spin-resolved spectral function at the Fermi energy $A_\sigma(0) \sim 1/\Gamma_\sigma \sim 1/(1 \pm P)$. This expectation is nicely confirmed by our numerical results in Fig. 9(a). As the $T = 0$ conductance is given by the product of $A_\sigma(0)$ and Γ_σ the spin-resolved conductance $G_\sigma \sim \Gamma_\sigma A_\sigma(0)$ becomes P independent. The results of the NRG calculation are shown in Fig. 9(b) confirming this expectation. We conclude that, even though one is dealing with spin-polarized leads, it is *not* possible to create a spin current via spin polarized leads the current remains spin independent. For the *a*ntiparallel alignment due to the DOS mismatch, the conductance will be reduced below $G_0 = 2e^2/h$ limit.

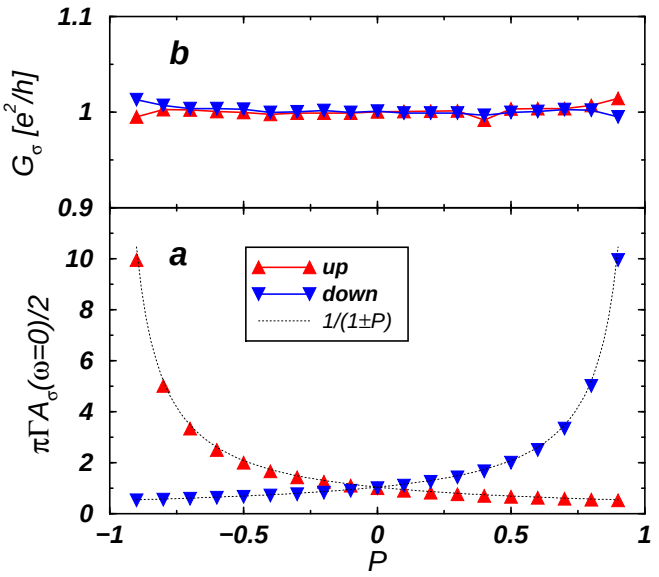

FIG. 9: (a) Height of the spin-resolved spectral function $A_\sigma(\omega = 0)$ as a function of P. The dashed line shows the $1/(1 \pm P)$ dependence as expected from the Friedel sum rule, Eq. (21). (b) Spin-resolved conductance G_σ as obtained from Eq. (23). This plot confirms the expectation based on the Friedel sum rule that the spin-resolved conductance should be independent of the spin species, consequently it serves as a consistency check of our numerics.

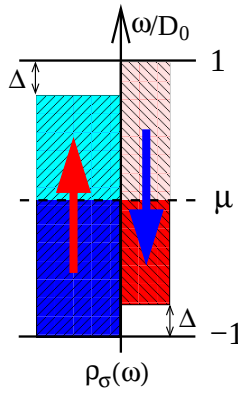

FIG. 10: The DOS in case of flat bands with the Stoner splitting Δ and a finite spin polarization P. In general the shifts of the $\uparrow$ and $\downarrow$ bands are unrelated to each other, $\Delta_\downarrow \neq -\Delta_\uparrow$. In this section, however, we assume $\Delta_\downarrow = -\Delta_\uparrow$.

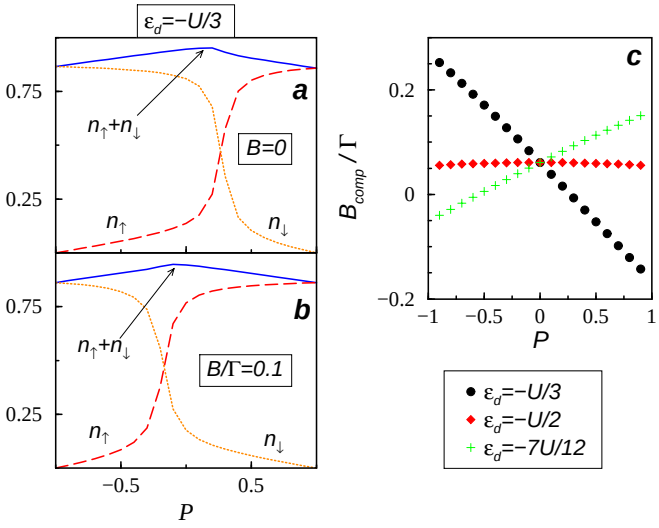

FIG. 11: Spin polarization P dependence of the local occupation n_σ for $B = 0$ (a) and $B = 0.1\ \Gamma$ (b) with $\epsilon_\mathrm{d} = -U/3$. The Stoner-splitting Δ even in the absence of spin polarization of the leads, $P = 0$, introduces an effective exchange field which splits the local level $n_\downarrow > n_\uparrow$ in absence of an external magnetic field $B = 0$. The spin polarization dependence of B_comp for various values of ϵ_d is shown in (c). To a good approximation the Stoner-splitting introduces a constant exchange field (here: $B_\mathrm{comp}/\Gamma \approx 0.061$), therefore it does nothing else but shifting the B_comp-dependence of section V. Parameters: $U = 0.12\left(\frac{D}{D_0}\right) D_0$, $\Gamma = U/6$, $\Delta_\downarrow = -\Delta_\uparrow = 0.10\left(\frac{D}{D_0}\right) D_0$.

VI. FLAT BANDS WITH STONER SPLITTING

In ferromagnetic leads, additional to a finite lead spin polarization P at the Fermi surface, a splitting between the spin-$\uparrow$ and spin-$\downarrow$ bands Δ_σ (Stoner splitting), which is effect of the effective exchange magnetic field in the leads, might appear. Taking this effect into account we do *not* expect the splitting of the Kondo resonance to disappear at $\epsilon_\mathrm{d} = -U/2$ as in Fig. 6(b), rather at a different value of ϵ_d determined by the shifts Δ_σ. This is due to the fact that the Stoner splitting breaks the particle-hole symmetry in the electrodes. Consequently we shall consider flat, spin-polarized leads (of polarization P), which are shifted relative to each other by an amount Δ_σ in this section. Since particle-hole symmetry is lost for this band structure in the leads we expect neither the splitting of the Kondo resonance, see e. g. Fig. 6, nor the compensation field B_comp to be symmetric around $\epsilon_\mathrm{d} = -U/2$, in contrast to Section V.

To quantify the statement that a shift Δ_σ introduces an finite exchange field and splitting, in this section we analyze the particular case $\Delta_\downarrow = -\Delta_\uparrow = \Delta$, sketched in Fig. 10. Note that the leads DOS structure discussed in this section[38] already requires the use of the extended NRG scheme, explained in Section III. In particular, spin-dependent on-site energies along the Wilson chain $\epsilon_{n\sigma}$, as explained in Section III and Appendix A and B, need to be determined to solve for the leads band structure shown in Fig. 10.

The studies summarized in Section V revealed that the spin-resolved impurity occupation n_σ is the key quantity in the context of a dot contacted to spin-polarized leads. Following this finding we plot n_σ vs. P for leads with $\Delta = 0.1\left(\frac{D}{D_0}\right) D_0$ and $\epsilon_\mathrm{d} = -U/3$ in Fig. 11. In contrast

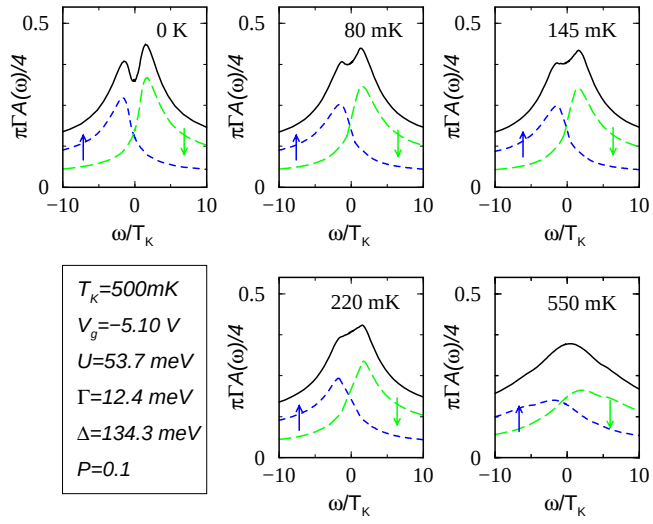

FIG. 12: Spin-resolved equilibrium spectral function $A_\sigma(\omega, T, V = 0)$ with parameters extracted from Ref. 11. The (blue) dashed lines correspond to $A_\uparrow(\omega, T, V = 0)$, the (green) long dashed lines to $A_\downarrow(\omega, T, V = 0)$ and the (red) solid ones to the sum of both, i. e. $A(\omega, T, V = 0)$. (a)-(e) A gradual increase in the temperature for those temperatures used in Ref. 11. For comparison we plot the $T = 0$ spectral function $A(\omega, T = 0, V = 0)$ in panel (a) as well. Note that the splitting of the Kondo resonance disappears upon increasing T.

to the previous section the impurity is preferably occupied by $\downarrow$-electrons in the absence of a magnetic field, see Fig. 11(a) even for $P = 0$. A finite magnetic field, e. g. $B/\Gamma = 0.1$ [Fig. 11(b)], has the same consequence as described before, namely the shift the local impurity levels $\epsilon_{\mathrm{d}\sigma}$. The P-dependence of B_{comp} for the particular band structure sketched in Fig. 10 is shown in Fig. 11(c); it is roughly given by the compensation field for flat bands, Fig. 5(a) where the same gate-voltages were used, shifted by an effective exchange field $\Delta\epsilon_{\mathrm{d}}^{(\mathrm{St})}$ generated by the band splittings for $P = 0$. The value of B_{Stoner} can be obtained via integrating out those band states of energy ω which lie in the interval $D \leq |\omega| \leq D_0$ (see Eq. (20). The value of this effective exchange field, which is logarithmically suppressed (as can be shown by perturbative scaling), given by Eq. (20). Inserting the numbers used in this section we obtain a $\Delta\epsilon_{\mathrm{d}}^{(\mathrm{St})}/\Gamma \approx 0.060$. The numerical calculation reveals $\Delta\epsilon_{\mathrm{d}}^{(\mathrm{St})}/\Gamma \approx 0.061$ [see Fig. 11(c)], i. e. the numerical result agrees reasonably well with the result based on scaling analysis (See Sec. IV).

A. Finite temperature: Comparison with experimental data

In a recent experiment of Nygård[11] *et al.* an anomalous splitting of the zero bias anomaly in the conductance induced by the Kondo resonance in *absence* of a magnetic field was observed. In this experiment quantum dot based on single wall carbon nanotubes (SWNT) contacted to non-magnetic, spin unpolarized Cr/Au electrodes were used. Those authors related the observed splitting of the Kondo resonance at zero magnetic field with the presence of a ferric iron nitrate nanoparticle[39], which due electronic tunnel coupling to the dot introduces a spin-dependent hybridization.

We model the setup of Ref. 11 by means of a single-level dot tuned to the local moment regime $\epsilon_{\mathrm{d}\sigma} = -U/2$ [dashed line in Fig. 1(b) of Ref. 11]. Moreover we used $T_{\mathrm{K}} = 500$ mK[40], which is in roughly the value of T_{K} observed in Ref. 11, as an input parameter and extracted from this value $U/\Gamma = 4.3$. Since a splitting of the Kondo resonance was observed for $\epsilon_{\mathrm{d}\sigma} = -U/2$, see e.g. Fig. 1(b) of Ref.[11], a particle-hole asymmetry must exist to achieve a splitting. We try to model this effect by using flat band structure and by introducing the Stoner splitting. We find the best agreement between the experimentally observed splitting of the Kondo resonance for $\Delta/U = 2.5$. The presence of the nanoparticle introduces a spin-dependent hybridization which we parameterize via the leads spin polarization P.

The comparison of the dI/dV vs. V characteristics of Ref.[11] with the theoretical result turns out to be rather complicated as it involves the *nonequilibrium* spectral function $A(\omega, T, V)$ which itself is not known how to compute accurately.[41,42] It is possible to compare qualitatively the splitting in the non-equilibrium conductance obtained in the experiment to the single particle spectral function. Due to the splitting in the particle spectral function for the dot, that is strongly related with the low-bias conductance measurements we find close similarity between both of them. When we approximate the experimental results of dI/dV with $A(\omega, T, V = 0)$ we achieve the best agreement between theory and experiment for $P = 0.1$. For these parameters ($\epsilon_{\mathrm{d}\sigma} = -U/2$, $U/\Gamma = 4.3$, $\Delta/U = 2.5$ and $P = 0.1$) we compute the temperature dependent equilibrium spectral function $A(\omega, T, V = 0)$ presented in Fig. 12.

The numerical findings shown in Fig. 12 qualitatively confirm the behavior found in the experiment of Nygård and collaborators, namely vanishing splitting in the dI/dV curves upon with increasing temperature. In the experiment, however, the differential conductance dI/dV turns out to be asymmetric around the Fermi energy [see Fig. 2(b)-(e) in Ref. 11]. We attribute the asymmetry in the dI/dV curve with by the asymmetry in the coupling between left and right leads.

Finally we want to compare the temperature dependence of the linear conductance G found in Ref.[11] (see Fig. 2(a) of Ref.[11]), with the one based on the model described above. In absence of a magnetic field $B = 0$ and source-drain voltage $V = 0$ a plateau in G was found around $T \approx 500$ mK in the experiment. Note that the calculation of G does not involve the nonequilibrium spectral function so we can calculate it exactly. In Fig. 13(a) we show the theoretical curve of the spin-

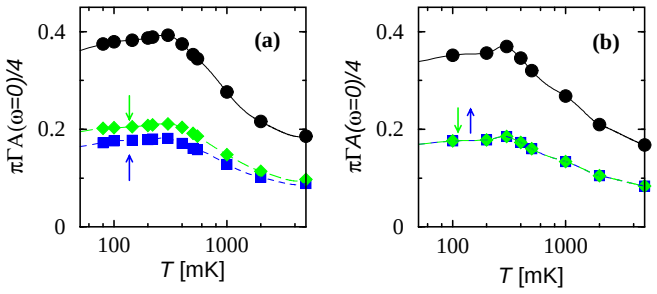

FIG. 13: Linear conductance as a function of temperature (a) for the model studied in this section and (b) for the case of a dot coupled to normal spin unpolarized leads ($P = 0$ and $\Delta = 0$) but in presence of a magnetic field $B = 0.02U$. In both cases a plateau in the linear conductance around T_K can be observed. Whereas the spin-resolved linear conductance is degenerate in case (b) (since it is the symmetric Anderson model with particle-hole symmetry), this is not the case for (a). Parameters as in Fig. 12, besides $P = \Delta = 0$ in case (b).

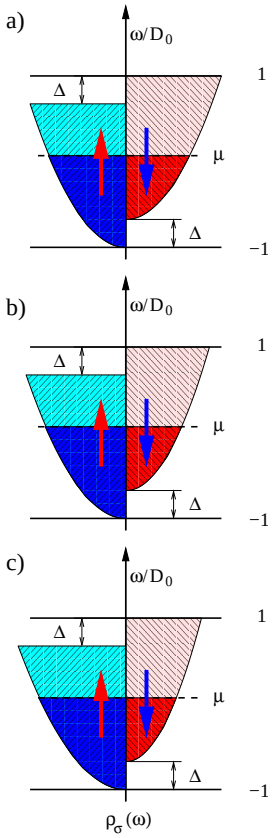

FIG. 14: The parabolic density of states (typical for s electron band) given by Eq. (24) with the same Stoner splitting $\Delta = 0.3D$ but with an additional spin asymmetry Q defined in the text. Here $Q = 0.0$ (a), 0.1 (b), and 0.3 (c).

resolved conductance G_σ obtained via Eq. (23) for the model discussed in this section. In agreement with the experiment a plateau in the linear conductance G is found around T_K.

For comparison we also plot the linear conductance of a dot contacted to normal spin unpolarized leads (i. e. flat bands with $P = 0$ which are not shifted relative to each other) for increasing temperature, however in *presence* of a finite magnetic field $B = 0.02\,U$ in Fig. 13(b). Such a magnetic field might e. g. be inserted in the system via the presence of the ferromagnetic nanoparticles. Also such a scenario leads to a plateau in G. The value of the associated magnetic field, however, is rather big $B = 0.02\,U$ corresponding to $B \approx 1$ T [here we assumed $g = 2.0$ for the conduction electrons in the nanotube (see also Ref. 11)]. According to Ref. 11 the latter scenario can therefore *not* explain the observed behavior, since one can argue that such a large magnetic field is hardly to believe can exist in this experiment (see in particular the footnote 13 of Ref.[11]).

Consequently, the presence of ferromagnetic leads might explain the experimental observation. We can, however, not exclude other possible mechanisms - such as the existence of an effective magnetic field - which might lead to the observed behavior, however, only form special geometry, where the strong stray magnetic field is possible.

VII. BAND STRUCTURE WITH ARBITRARY SHAPE

Flat bands, studied in the previous sections, are only a poor approximation of a realistic band-structure in the leads.[43] We complete our study by analyzing the effect of an *arbitrary* leads DOS. Consequently we are considering leads with a DOS which is energy- and spin-dependent, and additionally contains a Stoner splitting in this section. As outlined in the previous section the 'generalized' NRG-formalism introduced in Section III has to be used in this case as well. In particular, we study the effect of gate voltage variation on the spin-splitting of the local level of a quantum dot attached to ferromagnetic leads. We show how the gate voltage can control the magnetic properties of the dot. A similar proposal, namely to control the magnetic interactions via an electric field, was recently made in gated structures.[44]

In an analysis of several types of band structures we found three typical gate voltage dependences of the Kondo resonance. To be more specific, to illustrate this behavior we used a square-root shape DOS or parabolic band (as for free s-type electrons)[45] with the Stoner splitting Δ[46], and some additional spin asymmetry Q

$$\rho_\sigma(\omega) = \frac{1}{2}\frac{3\sqrt{2}}{8} D^{-3/2}(1+\sigma Q)\sqrt{\omega + D + \sigma\Delta/2} \quad (24)$$

depicted in Fig. 14 [$\sigma \equiv 1(-1)$ for $\uparrow$ ($\downarrow$)]. This example turns out to encompass three typical classes mentioned above. Note that we restricted the DOS in Eq. (24) $\omega \in [-D - \sigma\Delta/2, D - \sigma\Delta/2]$ to ensure that we are dealing with a normalized DOS.

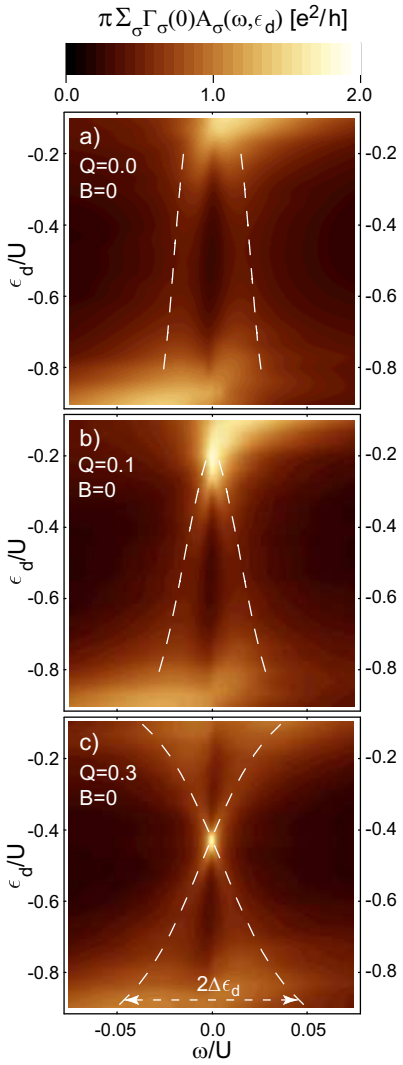

FIG. 15: Color scale plot of the (rescaled) spectral function $\sum_\sigma \Gamma_\sigma A_\sigma(\omega)$: the dashed lines mark the Kondo resonance for the leads band-structure as shown in Fig. 14 in absence of an external magnetic field. Whereas panel (a)-(c) correspond to a quantum dot in absence of an external magnetic field, in panel (d)-(f) an external field is applied.

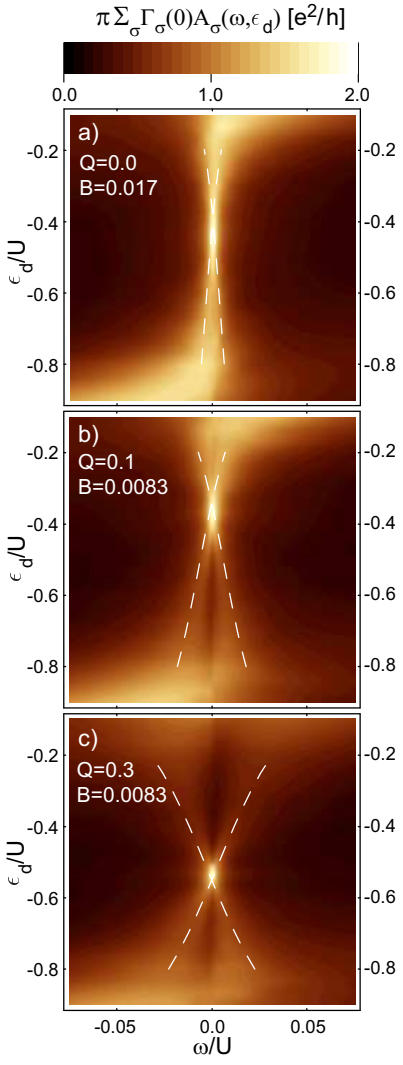

FIG. 16: Color scale plot of the (rescaled) spectral function $\sum_\sigma \Gamma_\sigma A_\sigma(\omega)$: the dashed lines mark the Kondo resonance for the leads band-structure as shown in Fig. 14. In contrast to Fig. 15 an external field is applied. As explained in Section V a local magnetic field shifts the spin-resolved local levels relative to each other leading to a change in the gate voltage where the compensation ($n_\uparrow = n_\downarrow$) takes place.

The three typical gate voltage dependences of the Kondo resonance we found: (i) a scenario where the splitting of the local level was roughly independent of gate voltage [Fig. 15(a)], (ii) a scenario with a strong gate voltage dependence of the splitting, however without compensation [Fig. 15(b)] and (iii) a case with a strong gate voltage dependence of the splitting including a particular gate voltage where the splitting vanishes [Fig. 15(c)]. Fig. 16(a), (b), and (c) shows the effect of an external magnetic field for Fig. 15(a), (b), and (c) respectively. As already outlined in the previous sections an external magnetic field can be used to compensate the lead induced spin-splitting (which itself depends on gate voltage) and thereby change that gate voltage where the full Kondo resonance exists, see Fig. 15(c) and Fig. 16(c).

The spitting of the spectral function (see Figs. 15 and 16) agrees very well with the splitting based on Haldane's scaling approach[16] given by the formula Eq. (17). The white dashed line in Figs. 15 and 16 shows prediction of Eq. (17), which fit very well to the numerical results presented.

In Fig. 17(a)-(c) we plot the linear conductance[47] G for the three band-structures sketched in Fig. 14 as a function of gate voltage ϵ_d and external magnetic field B. The two horizontal maxima in the conductance around $\epsilon_\mathrm{d} \approx 0$ and $\epsilon_\mathrm{d} \approx -U$ correspond to standard Coulomb resonances. The increased conductance in between, however, is due to the Kondo effect. Note that, in contrast to the Kondo effect observed in case of a dot attached to

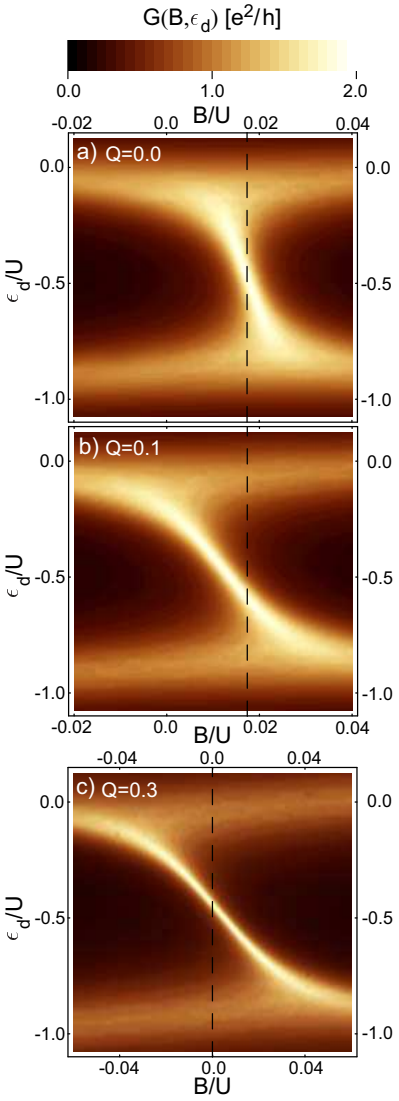

FIG. 17: Color scale plot of the linear conductance G as a function of gate voltage ϵ_d and magnetic field B for the band-structures corresponding to Fig. 14(a)-(c) [i. e. (a) corresponds to $Q = 0$, (b) to $Q = 0.1$ and (c) to $Q = 0.3$]. The black dashed line indicates cross-sections for which the amplitude is plotted in Fig. 19(b). Note the charging resonances around $\epsilon_d \approx 0$ and $\epsilon_d \approx -U$ and the tilted resonance (due to the Kondo effect) for $-U \lesssim \epsilon_d \lesssim 0$.

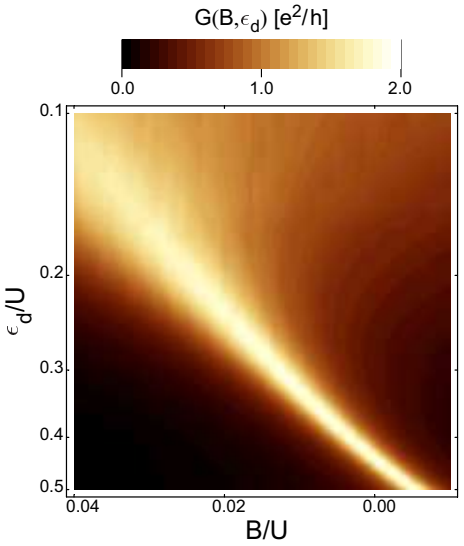

FIG. 18: Log-linear version of the Fig. 17(c) - color scale plot of the linear conductance G as a function of gate voltage ϵ_d and magnetic field B for the band-structures corresponding to Fig. 14(c).

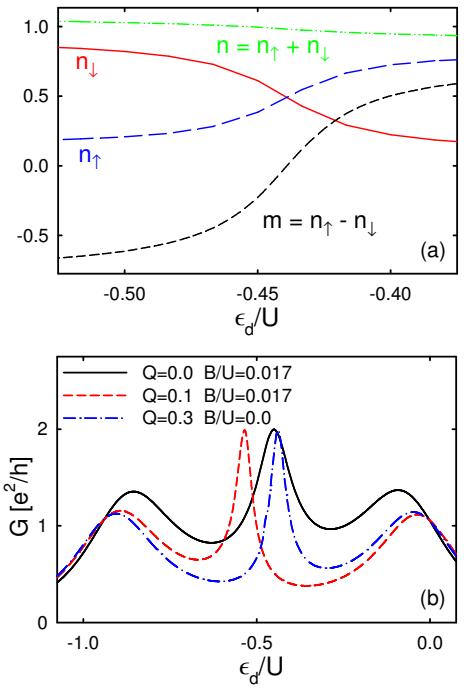

FIG. 19: The spin-resolved impurity occupation n_σ for the DOS reflecting Fig. 14(a) and Fig. 15(a) is plot in panel (a). It nicely illustrates that ϵ_d can be employed to tune the average impurity magnetization. Since the Kondo resonance is only fully recovered for $n_\uparrow = n_\downarrow$ the linear conductance G shows three peaks in panel (b) for three different situations corresponding to black dashed lines from Fig. 17.

flat and unpolarized leads (where the Kondo resonance is a vertical line), the Kondo resonance has a finite slope here. This is due to the gate voltage dependence (and correspondingly to the compensation field dependence) of the the spin splitting of the local level [Eq. (17)].

It is interesting to consider how the Kondo resonance merge with Coulomb resonances. As one can learn form Eq. (18) that the splitting $\delta\epsilon_d$ for the flat band structure without Stoner splitting shows a logarithmic divergence for $\epsilon_0 \to 0$ or $U + \epsilon_0 \to 0$. Since any sufficiently smooth DOS can be linearized around the Fermi surface, this logarithmic divergence occurs quite universally, as can be observed in log-linear versions of Fig. 17(c) demonstrated in Fig. 18. For finite temperature ($T > 0$) the logarithmic divergence for $\epsilon_0 \to 0$ or $\epsilon_0 \to -U$ is cut off, $\Delta\epsilon \simeq$

$-(1/\pi)P\Gamma[\Psi(1/2)+\ln(2\pi T/U)]$, which is also important for temperatures $T \ll T_{\rm K}$.

The finite slope of the Kondo resonance in the linear conductance plot motivates us to suggest an interesting possibility here: a dot attached to leads with a DOS as described in Eq. (24) and say $Q = 0.3$, see Fig. 17(c), the gate voltage can be used to tune the magnetization of the dot. In absence of an external magnetic field $B = 0$ the dot is not occupied by a preferred spin species for a particular gate voltage (which is $\epsilon_{\rm d} \approx -U/2$ in this case). Consequently the dot is preferably occupied with electrons of spin σ for $\epsilon_{\rm d} \gtrsim -U/2$ and electrons of opposite spin $\bar{\sigma}$ for $\epsilon_{\rm d} \lesssim -U/2$. In other words, the average spin on a dot contacted to leads with such a DOS, n_σ, and consequently its magnetization $m = n_\uparrow - n_\downarrow$ are tunable via an electric field, which in turn affects $\epsilon_{\rm d}$. This observation suggests the interesting possibility (similar to Ref. 44) to employ an electric field to tune the magnetic properties of a dot. To compute the gate voltage dependence of the magnetic field, of course, a detailed knowledge of the band-structure in the leads is necessary. Fig. 19(a) summarizes this discussion.

Another consequence of the leads band-structure is that the linear conductance G does not show a plateau when plotted relative to $\epsilon_{\rm d}$. Instead, we observe a three peak structure in G [see Fig. 19(b)] due to the particular gate voltage at which the full Kondo resonance is recovered.

The theoretical predictions made in this section were done for particular leads DOS of Eq. (24). We used this particular leads DOS to illustrate the effects on the spin-splitting of the local level triggered by the band-structure of the leads. To quantitatively compare our predictions with experiments, however, a detailed knowledge of the leads DOS is necessary which is in general very difficult to obtain.

VIII. CONCLUSION

We analyzed the effect of the band structure of the ferromagnetic leads on the spin splitting of the local level $\epsilon_{{\rm d}\sigma}$ of a quantum dot attached to them. We analyzed the effect of a finite spin polarization P in case of flat (energy-independent) bands. We found that the a finite lead polarization results in a spin splitting, of the local level and the Kondo resonance in a single particle spectral function, which can be compensated by an appropriately tuned magnetic field. Given the condition $n_\uparrow = n_\downarrow$ is recovered the isotropic Kondo effect is recovered even though the dot is contacted to leads with a finite spin polarization. Additional to this we identified that a finite Stoner splitting introduces an effective exchange field in the dot. Finally we explained the consequences of an energy- and spin-dependent band-structure on the local level. We confirmed that also in this general case the Kondo resonance can be recovered. From a methodological point of view we extended the 'standard' NRG procedure to treat leads with an energy- and spin-dependent DOS.

We thank J. Barnaś, T. Costi, L. Glazman, W. Hofstetter, B. Jones, C. Marcus, J. Nygård, A. Pasupathy, D. Ralph, A. Rosch, Y. Utsumi, and M. Vojta for discussions. This work was supported by the DFG under the CFN, 'Spintronics' RT Network of the EC RTN2-2001-00440, Projects OTKA D048665, T048782, SFB 631, and by the Polish grand for science in years 2006-2008 as a research project. Additional support from CeNS is gratefully acknowledged. L.B. is a grantee of the János Bolyai Scholarship. This research was also supported in part by the National Science Foundation under Grant No. PHY99-07949.

APPENDIX A: TRANSFORMATION OF TUNNELING HAMILTONIAN - $\hat{\mathcal{H}}_{\ell d}$

The continuous representation of the tunneling Hamiltonian $\hat{\mathcal{H}}_{\ell d}$, Eq. (3), can be rewritten in terms of discrete conduction band operators for each spin component separately by replacing the continuous conduction band operators $\alpha_{\omega\sigma}$ by discrete ones, as suggested in Eq. (10)

$$\hat{\mathcal{H}}_{\ell d} = \sum_{np\sigma}\left[d_\sigma^\dagger \left(a_{np\sigma} \int_{\Lambda^{-(n+1)}}^{\Lambda^{-n}} d\omega\; h_\sigma(\omega)\Psi_{np}^+(\omega) + \right.\right. \\ \left.\left. + b_{np\sigma} \int_{-\Lambda^{-n}}^{-\Lambda^{-(n+1)}} d\omega\; h_\sigma(\omega)\Psi_{np}^-(\omega) \right) + \text{h.c.} \right] . \quad \text{(A1)}$$

As outlined in Section III we replace the energy dependent generalized hybridization of the n-th logarithmic interval $h_\sigma(\omega)$, $\Lambda^{-(n+1)} \pm \omega < \Lambda^{-n}$, by a constant $h_{n\sigma}^\pm$, defined as

$$h_{n\sigma}^+ \equiv \begin{cases} \frac{1}{d_n}\int_{\Lambda^{-(n+1)}}^{\Lambda^{-n}} d\omega \sqrt{\rho_\sigma(\omega)\left[V_\sigma(\omega)\right]^2} & \text{if } \Lambda^{-(n+1)} \le \omega < \Lambda^{-n} \\ 0 & \text{else} \end{cases}$$

$$h_{n\sigma}^- \equiv \begin{cases} \frac{1}{d_n}\int_{-\Lambda^{-n}}^{-\Lambda^{-(n+1)}} d\omega \sqrt{\rho_\sigma(\omega)\left[V_\sigma(\omega)\right]^2} & \text{if } -\Lambda^{-n} < \omega \le -\Lambda^{-(n+1)} \\ 0 & \text{else} \end{cases} .$$

Consequently possible integrals in Eq. (A1), such as $\int_{\Lambda^{-(n+1)}}^{\Lambda^{-n}} d\omega\; h_\sigma(\omega)\Psi_{np}^+(\omega) \propto \int_{\Lambda^{-(n+1)}}^{\Lambda^{-n}} d\omega \Psi_{np}^+(\omega)$, give only for $p = 0$ (due to the Riemann-Lebesgue Lemma) a fi-

nite contribution. For the particular choice of constant hybridization the impurity couples to s-waves ($p = 0$ modes) only; consequently we skip the harmonic index p below. With above definitions Eq. (A1) simplifies to the following compact form

$$\hat{\mathcal{H}}_{\ell d} = \frac{1}{\sqrt{\pi}} \sum_{\sigma} \left[d_{\sigma}^{\dagger} \sum_{n} \left(a_{n\sigma} \gamma_{n\sigma}^{+} + b_{n\sigma} \gamma_{n\sigma}^{-} \right) + \text{h.c.} \right], \tag{A2}$$

where

$$\begin{aligned} \gamma_{n\sigma}^{+} &\equiv \int_{\Lambda^{-(n+1)}}^{\Lambda^{-n}} d\omega \, \sqrt{\pi \rho_{\sigma}(\omega) \left[V_{\sigma}(\omega) \right]^2} \\ \gamma_{n\sigma}^{-} &\equiv \int_{-\Lambda^{-n}}^{-\Lambda^{-(n+1)}} d\omega \, \sqrt{\pi \rho_{\sigma}(\omega) \left[V_{\sigma}(\omega) \right]^2} \, . \end{aligned} \tag{A3}$$

Remember that Eq. (9) forces the generalized dispersion $g_{\sigma}(\epsilon)$ to be adjusted accordingly for this particular choice of $h_{\sigma}(\omega)$. It is explained in details in Appendix B.

APPENDIX B: MAPPING OF CONDUCTION BAND ONTO SEMI-INFINITE CHAIN

Here we outline the important steps to bring the leads Hamiltonian $\hat{\mathcal{H}}_{\ell}$, Eq. (8), into the tridiagonal from introduced in Eq. (13). The replacement of the continuous conduction band operators $\alpha_{\omega\sigma}$ by discrete operators, cf. Eq. (10), simplifies $\hat{\mathcal{H}}_{\ell}$ significantly.[48] As shown in Ref. 27 the particular choice of the generalized hybridization function $h_{\sigma}(\omega) \to h_{n\sigma}^{\pm}$ (given in Appendix A) results in

$$\hat{\mathcal{H}}_{\ell} = \sum_{n\sigma} \left[\zeta_{n\sigma}^{+} a_{n\sigma}^{\dagger} a_{n\sigma} + \zeta_{n\sigma}^{-} b_{n\sigma}^{\dagger} b_{n\sigma} \right], \tag{B1}$$

where

$$\zeta_{n\sigma}^{+} \equiv \frac{\int_{\Lambda^{-(n+1)}}^{\Lambda^{-n}} d\epsilon \, \epsilon \, \rho_{\sigma}(\epsilon)}{\int_{\Lambda^{-(n+1)}}^{\Lambda^{-n}} d\epsilon \, \rho_{\sigma}(\epsilon)} \, , \tag{B2}$$

$$\zeta_{n\sigma}^{-} \equiv \frac{\int_{-\Lambda^{-n}}^{-\Lambda^{-(n+1)}} d\epsilon \, \epsilon \, \rho_{\sigma}(\epsilon)}{\int_{-\Lambda^{-n}}^{-\Lambda^{-(n+1)}} d\epsilon \, \rho_{\sigma}(\epsilon)} \, . \tag{B3}$$

To achieve the goal to bring $\hat{\mathcal{H}}_{\ell}$ into tridiagonal form the tridiagonalization procedure developed by Lánczos[30] is used. In general diagonal and off-diagonal matrix elements $\epsilon_{n\sigma}$ and $t_{n\sigma}$[49] need to be computed in the course of the procedure. These matrix elements can be obtained by demanding the following relation (see e.g. Ref. 17)

$$\begin{aligned} &\sum_{n\sigma} \left(\zeta_{n\sigma}^{+} \, a_{n\sigma}^{\dagger} a_{n\sigma} + \zeta_{n\sigma}^{-} \, b_{n\sigma}^{\dagger} b_{n\sigma} \right) = \\ &\quad = \sum_{n\sigma} \left[\epsilon_{n\sigma} f_{n\sigma}^{\dagger} f_{n\sigma} + t_{n\sigma} \left(f_{n\sigma}^{\dagger} f_{n+1\sigma} + f_{n+1\sigma}^{\dagger} f_{n\sigma} \right) \right]. \end{aligned} \tag{B4}$$

The spin-dependent coefficients $u_{nm\sigma}$ and $v_{nm\sigma}$ of the single-particle operator [Eq. (15)] (that acts on the n-th site of the Wilson chain) $f_{n\sigma}$, given by the Ansatz Eq. (14), need to be determined recursively for each spin component separately. Inverting the Ansatz Eq. (14) enables one to express the discrete conduction band operators as $a_{n\sigma} = \sum_{m=0}^{\infty} u_{mn\sigma} f_{m\sigma}$ and $b_{n\sigma} = \sum_{m=0}^{\infty} v_{mn\sigma} f_{m\sigma}$, respectively. When we insert $a_{n\sigma}$ and $b_{n\sigma}$ in the l.h.s. of Eq. (B4) and compare corresponding $f_{n\sigma}$ operators on both sides of this equation we obtain

$$\begin{aligned} &\sum_{m=0}^{\infty} \left(\zeta_{ms}^{+} u_{nm\sigma} a_{m\sigma}^{\dagger} + \zeta_{ms}^{-} v_{nm\sigma} b_{m\sigma}^{\dagger} \right) = \\ &\qquad = \epsilon_{n\sigma} f_{n\sigma}^{\dagger} + t_{n\sigma} f_{n+1\sigma}^{\dagger} + t_{n-1\sigma} f_{n-1\sigma}^{\dagger} \, . \end{aligned} \tag{B5}$$

In particular, Eq. (B5) for $n = 0$ gives the relation for the operators $f_{0\sigma}$ yields

$$\begin{aligned} &\sum_{m=0}^{\infty} \left(\frac{\zeta_{m\sigma}^{+} \gamma_{m\sigma}^{+}}{\sqrt{\xi_{0\sigma}}} a_{m\sigma}^{\dagger} + \frac{\zeta_{m\sigma}^{-} \gamma_{m\sigma}^{-}}{\sqrt{\xi_{0\sigma}}} b_{m\sigma}^{\dagger} \right) \\ &\qquad = \epsilon_{0\sigma} f_{0\sigma}^{\dagger} + t_{0\sigma} f_{1\sigma}^{\dagger}, \end{aligned} \tag{B6}$$

where the corresponding values of $u_{0m\sigma}$ and $v_{0m\sigma}$ [Eq. (15)] have already been inserted. Since the operators $f_{n\sigma}$ obey Fermi-statistics, $\{ f_{n\sigma}, f_{n'\sigma'}^{\dagger} \} = \delta_{nn'} \delta_{\sigma\sigma'}$, the anticommutator of the r.h.s. of Eq. (B6) with $f_{0\sigma}$ yields $\{ \epsilon_{0\sigma} f_{0\sigma}^{\dagger} + t_{0\sigma} f_{1\sigma}^{\dagger}, f_{0\sigma} \} = \epsilon_{0\sigma}$. The corresponding anticommutator of the l.h.s. of Eq. (B6) with $f_{0\sigma}$ finally results in

$$\epsilon_{0\sigma} = \frac{1}{\xi_{0\sigma}} \sum_{m} \left[\zeta_{m\sigma}^{+} \left(\gamma_{m\sigma}^{+} \right)^2 + \zeta_{m\sigma}^{-} \left(\gamma_{m\sigma}^{-} \right)^2 \right]. \tag{B7}$$

The initial hopping matrix element $t_{0\sigma}$ is readily obtained from the anticommutator $\{ \epsilon_{0\sigma} f_{0\sigma}^{\dagger} + t_{0\sigma} f_{1\sigma}^{\dagger}, \epsilon_{0\sigma} f_{0\sigma} + t_{0\sigma} f_{1\sigma} \} = (\epsilon_{0\sigma})^2 + (t_{0\sigma})^2$. As $\epsilon_{0\sigma}$ is known, $t_{0\sigma}$ can be easily obtained from Eq. (B6)

$$\begin{aligned} (t_{0\sigma})^2 = \Bigg\{ &\sum_{m} \left[\left(\zeta_{m\sigma}^{+} \right)^2 \left(\gamma_{m\sigma}^{+} \right)^2 + \left(\zeta_{m\sigma}^{-} \right)^2 \left(\gamma_{m\sigma}^{-} \right)^2 \right] - \\ &\sum_{m} \left[\zeta_{m\sigma}^{+} \left(\gamma_{m\sigma}^{+} \right)^2 + \zeta_{m\sigma}^{-} \left(\gamma_{m\sigma}^{-} \right)^2 \right] \Bigg\} \Big/ \xi_{0\sigma} \end{aligned} \tag{B8}$$

The knowledge of $\epsilon_{0\sigma}$, $t_{0\sigma}$, and $f_{0\sigma}$ now enables us to extract the coefficients of $f_{1\sigma}$ from Eq. (B6)

$$\begin{aligned} u_{1m\sigma} &= \frac{\gamma_{m\sigma}^{+}}{\sqrt{\xi_{0\sigma}} t_{0\sigma}} \left(\zeta_{m\sigma}^{+} - \epsilon_{0\sigma} \right) \, , \\ v_{1m\sigma} &= \frac{\gamma_{m\sigma}^{-}}{\sqrt{\xi_{0\sigma}} t_{0\sigma}} \left(\zeta_{m\sigma}^{-} - \epsilon_{0\sigma} \right) \, . \end{aligned} \tag{B9}$$

A generalization of the argumentation above finally allows one to obtain the spin-dependent on-site energies $\epsilon_{n\sigma}$ and hopping matrix elements $t_{n\sigma}$ for the n-th site of the Wilson chain

$$\epsilon_{n\sigma} = \sum_{m} \left[(u_{nm\sigma})^2 \zeta_{m\sigma}^{+} + (v_{nm\sigma})^2 \zeta_{m\sigma}^{-} \right], \tag{B10}$$

$$\begin{aligned} (t_{n\sigma})^2 = &\sum_{m} \left[(u_{nm\sigma})^2 \left(\zeta_{m\sigma}^{+} \right)^2 + (v_{nm\sigma})^2 \left(\zeta_{m\sigma}^{-} \right)^2 \right] \\ &- (t_{n-1\sigma})^2 - (\epsilon_{n\sigma})^2 \, , \end{aligned} \tag{B11}$$

where the involved coefficients of the single-particle operator $f_{n+1\sigma}$, are given as

$$\begin{aligned} u_{n+1m\sigma} &= \frac{1}{t_{n\sigma}}\left[\left(\zeta^{+}_{m\sigma}-\epsilon_{n\sigma}\right)u_{nm\sigma}-t_{n-1\sigma}u_{n-1m\sigma}\right] , \\ v_{n+1m\sigma} &= \frac{1}{t_{n\sigma}}\left[\left(\zeta^{-}_{m\sigma}-\epsilon_{n\sigma}\right)v_{nm\sigma}-t_{n-1\sigma}v_{n-1m\sigma}\right] . \end{aligned} \tag{B12}$$

Note that it is crucial to determine the coefficients $u_{nm\sigma}$ and $v_{nm\sigma}$ even though, only the matrix elements along the Wilson chain ($\epsilon_{n\sigma}$ and $t_{n\sigma}$) are finally required. The numerical solution of the above mentioned equations is rather tricky: since the band energies are exponentially decaying in the course of the iteration one has to use reliable numerical routines (i.e. arbitrary-precision Fortran routines[27]) to solve for the coefficients $u_{nm\sigma}$ and $v_{nm\sigma}$ and the matrix elements $t_{n\sigma}$ or $\epsilon_{n\sigma}$, respectively.

[1] M. R. Buitelaar, T. Nussbaumer, and C. Schönenberger, Phys. Rev. Lett. **89**, 256801 (2002).

[2] N. Sergueev, Q. Sun, H. Guo, B.G. Wang, and J. Wang, Phys. Rev. B **65**, 165303 (2002).

[3] P. Zhang, Q. Xue, Y. Wang, and X.C. Xie, Phys. Rev. Lett. **89**, 286803 (2002).

[4] B. R. Bulka and S. Lipiński, Phys. Rev. B **67**, 024404 (2003).

[5] R. Lopez and D. Sánchez, Phys. Rev. Lett. **90**, 116602 (2003).

[6] J. Martinek, Y. Utsumi, H. Imamura, J. Barnaś, S. Maekawa, J. König, and G. Schön, Phys. Rev. Lett. **91**, 127203 (2003).

[7] J. Martinek, M. Sindel, L. Borda, J. Barnaś, J. König, G. Schön, and J. von Delft, Phys. Rev. Lett. **91**, 247202 (2003).

[8] M. S. Choi, D. Sánchez, and R. López, Phys. Rev. Lett. **92**, 056601 (2004).

[9] Y. Utsumi, J. Martinek, G. Schön, H. Imamura, and S. Maekawa, Phys. Rev. B **71**, 245116 (2005).

[10] A. N. Pasupathy, R. C. Bialczak, J. Martinek, J. E. Grose, L. A. K. Donev, P. L. McEuen, and D. C. Ralph, Science **306**, 86 (2004).

[11] J. Nygård, W. F. Koehl, N. Mason, L. DiCarlo, and C. M. Marcus, cond-mat/0410467 (2004).

[12] S. Maekawa and T. Shinjo, *Spin Dependent Transport in Magnetic Nanostructures*, Taylor & Francis (2002); S. Maekawa ed. *Concepts in Spin Electronics* Oxford (2005).

[13] J. Martinek, M. Sindel, L. Borda, J. Barnas, R. Bulla, J. König, G. Schön, S. Maekawa, J. von Delft, Phys. Rev. B **72**, R121302 (2005).

[14] K. G. Wilson, Rev. Mod. Phys. **47**, 773 (1975).

[15] P. W. Anderson, J. Phys. C, **10**, 3589 (1977).

[16] F. D. M. Haldane, Phys. Rev. Lett. **40**, 416 (1978).

[17] R. Bulla, H. - J. Lee, N. - H. Tong, and M. Vojta, Phys. Rev. B **71**, 045122 (2005).

[18] We use normalized density of statets in the leads, $\sum_{r\sigma}\int_{-\infty}^{\infty} d\omega\rho_{r\sigma}(\omega)=1$, throughout this report.

[19] L. I. Glazman and M. E. Raikh, JETP Lett. **47**, 452 (1988); T. K. Ng and P. A. Lee, Phys. Rev. Lett. **61**, 1768 (1988).

[20] W. Nolting, A. Vega, and T. Fauster, Z. Phys. B **96**, 357 (1995).

[21] E. Yu. Tsymbal and D. G. Pettifor, J. Phys.:Condens. Matter **9**, L411 (1997).

[22] We expect that a finite s-electron interaction, $U_s > 0$, will lead only to a slight renormalization of $T_{\rm K}$.

[23] J. König and J. Martinek, Phys. Rev. Lett. **90**, 166602 (2003); M. Braun, J. König, and J. Martinek, Phys. Rev. B **70**, 195345 (2004); J. König, J. Martinek, J. Barnaś, and G. Schön, Lecture Notes in Physics **658**, Springer, 145-164 (2005).

[24] H. R. Krishna-murthy, J. W. Wilkins and K. G. Wilson, Phys. Rev. B, **21**, 1003 (1980); Phys. Rev. B, **21**, 1044 (1980).

[25] T. A. Costi, A. C. Hewson, and V. Zlatic, J. Phys.: Cond. Matt. **6**, 2519 (1994).

[26] W. Hofstetter, Phys. Rev. Lett. **85**, 1508 (2000).

[27] R. Bulla, Th. Pruschke, A.C. Hewson, J. Phys. Cond. Matter, **9**, 10463 (1997).

[28] Krishna-murthy[24] *et al.* generalized the original mapping of Wilson[14] done for the Kondo model to a mapping of the Anderson model on the Wilson chain; still, however, with a constant leads DOS.

[29] Note that we are dealing with $V_\sigma(\omega) = V$, i.e. spin- and energy-independent tunneling matrix elements, in this section.

[30] C. Lánczos, J. Res. Natl. Bur. Stand., **45**, 255 (1950).

[31] W. Hofstetter and H. Schoeller, Phys. Rev. Lett. **88**, 016803 (2002).

[32] The spin-dependent DOS in case of flat and spin-polarized bands (with spin-polarization parameter P) is given by $\rho_\sigma = \frac{1}{2}\rho(1 \pm P)$, where $\rho = \frac{1}{2D}$ is the corresponding normalized DOS of the full band.

[33] T. A. Costi, Phys. Rev. Lett. **85**, 1504 (2000); Phys. Rev. B **64**, 241310 (2001).

[34] D. C. Langreth, Phys. Rev. **150**, 516 (1966).

[35] A. C. Hewson, *The Kondo Problem to Heavy Fermions*, Cambridge Univ. Press (1993).

[36] For a single level Anderson model the phase of the retarded Green's function is identical to the scattering phase.

[37] Note that in case of spin-polarized leads the condition $n_\uparrow = n_\downarrow$ is not identical to the condition of degenerate levels, as $\Gamma_\uparrow \neq \Gamma_\downarrow$.

[38] Note that the appearance of the Stoner splitting makes the use of the generalized bandwidth D_0 ($\neq D$) necessary.

[39] These nanoparticles act as catalyst for the growth of the nanotube on the SiO_2 substrate.

[40] The value of $T_{\rm K}$ was confirmed in a private communication with J. Nygård and C. M. Marcus.

[41] J. Paaske, A. Rosch, J. Kroha, and P. Wölfle, Phys. Rev. B **70**, 155301 (2004).

[42] To extract the *equilibrium* spectral function from a measurement is a nontrivial as well. There have been different proposals to achieve this. One can either use very asymmetric couplings to the leads, use a three terminal geometry [see E. Lebanon and A. Schiller, Phys. Rev. B **65**, 035308

(2002)] or extract $A_{\rm eq}$ from the frequency dependent conductance or noise [see M. Sindel, W. Hofstetter, J. von Delft, and M. Kindermann, Phys. Rev. Lett **94**, 196602 (2005)].

[43] D. A. Papaconstantopoulos, ed., *Handbook of the Band Structure of Elemental Solids*, Plenum Press (1986).

[44] H. Ohno, D. Chiba, F. Matsukura, T. Omiya, E. Abe, T. Dietl, Y. Ohno, K. Ohtani, Nature (London) **408**, 944 (2000). D. Chiba, M. Yamanouchi, F. Matsukura, and H. Ohno, Science **301**, 943 (2003).

[45] The DOS $\rho_\sigma(\omega)$ is defined as $\rho_\sigma(\omega) = \sum_k \delta(\omega - \epsilon_{k\sigma})$. Since free electrons have a dispersion $\epsilon_{k\sigma} = \frac{\hbar^2 k^2}{2m}$ one obtains $\rho_\sigma(\omega) \sim \int \sqrt{\omega'} d\omega' \delta(\omega - \omega') = \sqrt{\omega}$.

[46] K. Yosida, *Theory of Magnetism*, Springer (1996).

[47] We obtain the linear conductance $G(\epsilon_{\rm d}, B) = \sum_\sigma G_\sigma(\epsilon_{\rm d}, B)$, see Eq. (23), by computing the spin-resolved spectral function $A_\sigma(\omega = 0, \epsilon_{\rm d}, B)$ (for $T = 0$) for those values of $\epsilon_{\rm d}$ and B that are relevant for Fig. 16.

[48] M. Sindel, *Numerical Renormalization Group studies of Quantum Impurity Models in the Strong Coupling Limit*, PhD thesis, Munich (2005).

[49] W. Hofstetter, *Renormalization Group Methods for Quantum Impurity Systems*, PhD thesis, Augsburg (2000), ISBN 3-8265-8007-9 (Shaker Verlag, Aachen).